AN ABSTRACT OF THE THESIS OF

James A. Vanderwaal for the degree of Master of Science

in Forest Engineering presented on December 10, 1982

Title: Energy Exchange of Transplanted Douglas-fir Seedlings on Two Cutover Sites in Southwestern Oregon

Abstract approved: H. Richard Holbo

An energy balance analysis was performed on each of four transplanted Douglas-fir [Pseudotsuga menziesii (Mirb.) Franco] seedlings growing on two cutover sites in southwestern Oregon. The two sites were a clearcut and a partial-cut (shelterwood) side by side, with a pair of seedlings used on each site. One seedling of each pair had a shadecard to the southwest of that seedling. This way, the shelterwood harvest system and the use of shadecards were compared in relation to their success in ameliorating the microclimate of the seedlings.

A model of seedling radiation geometry was used along with measurements of site radiation and environmental temperatures to calculate the net radiation "loading" upon each seedling. This heat load was then partitioned into the two major heat dissipation modes, latent heat (transpiration) and sensible heat convection.

The resulting values of incident solar radiation, Bowen ratios, and water use calculations show that the partial-cut was more successful than the shadecards in improving the microclimate of the

transplanted seedlings and, therefore, increasing the chance of survival during periods of heat and moisture stress.

For August 7, 1981, the partial-cut was found to have reduced the daily solar radiation incident to a seedling by 29%. This compares to a reduction of 22% by a shadecard alone, and 47% by a partial-cut/shadecard combination. The partial-cut was, therefore, slightly more effective, in a quantitative sense, than a shadecard in reducing the amount of solar radiation incident to a seedling.

The Bowen ratio increased greatly throughout the summer for the two seedlings on the clearcut, but very little for the two seedlings on the partial-cut. By late August, the seedlings in the clearcut had a sensible-to-latent heat loss ratio of between 40- and 60-to-1 while the seedlings in the partial-cut had ratios of only 10- and 15-to-1. There was a greater difference in the clearcut/partial-cut comparison than in either of the shadecard/no card comparisons. This indicates that the residual canopy of the partial-cut had a large effect upon the Bowen ratio, while the shadecard had little effect upon the Bowen ratio on either site.

The water use by the seedlings on the clearcut changed markedly over the summer with the greatest use in May and the least use in August. In contrast, the two seedlings in the partial-cut had the lowest use in May, with greater use in either July or early August. The early August period coincided with one of the worst "heat waves" on record and this may have helped magnify the differences between treatments. As with the Bowen ratio, there was a greater difference between water uses in the clearcut/partial-cut comparison than in either of the shadecard/no card comparisons.

There was a significant difference in total water use between the two sites. The seedlings on the clearcut used about half the amount of water that the seedlings on the partial-cut used. There was also a great difference in distribution of water use. For example, the seedlings on the clearcut used between 47 and 54% of their total summer water use in the May to July period compared to only 31 to 39% for the seedlings in the partial-cut. In contrast, the clearcut seedlings used only 10 to 12% of total water use in late August when the partial-cut seedlings used 18 to 23%. This suggests that the seedlings in the clearcut were not as active in water use as those in the partial-cut in the late summer. This may be a result of the clearcut seedlings being water stressed from a lack of available water.

Energy Exchange of Transplanted Douglas-fir Seedlings on Two Cutover Sites in Southwestern Oregon

by

James A. Vanderwaal

A THESIS

submitted to

Oregon State University

in partial fulfillment of
the requirements for the
degree of
Master of Science

Commencement June 1983

ACKNOWLEDGEMENTS

This research was supported as part of the Forestry Intensified Research Program in southwest Oregon, which is cooperatively sponsored by the USDA Forest Service (Rogue, Siskiyou, and Umpqua National Forests and the Pacific Northwest Forest and Range Experiment Station) and by the USDI Bureau of Land Management (Medford and Roseburg Districts).

I take this opportunity to thank the members of my graduate committee, Drs. R. Dennis Harr, David R. DeYoe, and Dale E. Kirk, for a challenging thesis defense and for a very positive critique of the following manuscript.

I thank Dr. Stuart W. Childs for assisting with field measurements, data processing, providing much humor and lending me his spare banjo.

I also thank Edward L. Miller for his technical supervision and patience in answering a barrage of questions.

Special gratitude goes to Dr. H. Richard Holbo for giving me the opportunity to do this research, for teaching me much about environmental instrumentation and for an amiable personality.

Finally, I thank the Lord Jesus Christ, my wife, Jeanne Marie, and members of Corvallis Christian Center for love and support.

TABLE OF CONTENTS

	Page
INTRODUCTON	1
OBJECTIVES	4
Energy Balance Theory	5
The Study Sites	9
Site Data	11
Seedling Response Data	13
METHODS	19
RESULTS AND DISCUSSION	21
Comparison Between Geometrical Shapes	23
Partitioning of Net Radiation	25
Error in Energy Balance Measurements	28
Bowen Ratios	31
Diurnal Patterns of β and LE (Water Use)	34
Summer Pattern of Water Use	39
Water Use During Heat Wave Event	45
Applications to Reforestation	51
CONCLUSIONS	55
REFERENCES CITED	58
APPENDIX A	63
APPENDIX B	85
APPENDIX C	96
APPENDIX D	98

LIST OF FIGURES

Figure		Page
1.	Incoming solar radiation (K↓) to Douglas-fir seedlings on August 7, 1981.	22
2.	Incoming solar radiation (K↓) normalized to maximum half-hour value for a Douglas-fir seedling (CN), a spherical PAR sensor, and a horizontally-oriented pyranometer for data collected August 7, 1981.	24
3.	Net radiation (Q*) partitioning into sensible heat flux (H) and latent heat flux (LE) for seedling CN on May 28, 1981, and August 7, 1981.	27
4.	Seasonal trend in the Bowen ratio for four Douglas-fir seedlings on two cutover sites in southwest Oregon in 1981.	32
5.	Daily pattern in the Bowen ratio for seedlings CN and CS on August 7, 1981.	35
6.	Daily pattern in the Bowen ratio for seedlings PN and PS on August 7, 1981.	36
7.	Daily pattern in water use of seedlings CN and CS on August 7, 1981.	37
8.	Daily pattern in water use of seedlings PN and PS on August 7, 1981.	38
9.	Seasonal trend in water use of four Douglas-fir seedlings on two cutover sites in southwest Oregon in summer of 1981.	40
10.	Mean daily water use of four seedlings for the summer of 1981.	42
11.	Total water use of four seedlings for the summer of 1981.	43
12.	Stomatal resistance patterns of seedlings on the clear-cut with shadecards (S) and without shadecards (N) on August 7, 1981.	48
13.	Stomatal resistance patterns of seedlings on the partial-cut with shadecards (S) and without shadecards (N) on August 7, 1981.	49

Figure		Page
A1-3.	Douglas-fir seedling radiation geometry. A1 - seedling conceptualized as an assemblage of cylinders, A2 - incoming solar radiation geometry for the mainstem, A3 - incoming solar radiation geometry for a sidebranch.	64
A4.	Geometrical determination of when a sidebranch is shaded by the mainstem.	67
A5.	Horizontal shading geometry of a sidebranch.	68
A6.	Vertical shading geometry of a sidebranch.	70
A7.	Photograph of branch at $\alpha = 0°$. Used in determination of A_n/LA.	72
A8.	Photograph of branch at $\alpha = 90°$. Used in determination of A_n/LA.	72
A9.	The factor A_n/LA versus angle ALPHA (α) of the four branches (A, B, C, D) used to compute the regression line (R).	73
A10.	Vertical shading geometry of the shadecard upon a seedling.	77
A11.	Horizontal shading geometry of the shadecard upon a seedling.	79
A12.	Longwave view factors of each of the four seedlings used in energy balance calculations.	82

LIST OF TABLES

Table		Page
1.	Schedule of measurements for leaf temperature (T_ℓ), stomatal resistance (r_S), and site variables used in energy balance calculations. May 22, JD 142; July 2, JD 183; August 4, JD 217; and August 25, JD 237.	17
2.	Total leaf area (cm^2) of the four seedlings for each of four site visits. Treatment abbreviations are: C = clearcut, P = partial-cut, N = no card, and S = shadecard.	18
3.	Mean daily half-hour values of net radiation (Q*), sensible heat flux (H), latent heat flux (LE), and the Bowen ratio (β) for all four seedlings on the four selected days in the summer of 1981.	29
4.	Relative probable error in the energy balance terms.	30
5.	Fractional distribution of water use occurring within each of three summer periods.	46
D1.	Relative probable error in seedling CN latent heat flux (LE).	107
D2.	Relative probable error in seedling CN net radiation (Q*).	107
D3.	Relative probable error in seedling CN Bowen ratio (β).	108
D4.	Relative probable error in seedling CN convective heat flux (H).	108

LIST OF SYMBOLS

A	Total needle surface area (cm^2).
C_p	Specific heat of air (1.01 kJ/kg °C).
d	Characteristic dimension (diameter of cylinders) (m).
G	Sensible heat loss by conduction (W/m^2).
H	Sensible heat loss by convection (W/m^2).
J	Change in stored heat energy (W/m^2).
$K\downarrow$	Incoming solar (shortwave) radiation (W/m^2).
$K\uparrow$	Outgoing solar radiation (W/m^2).
$L\downarrow$	Incoming longwave radiation (W/m^2).
$L\uparrow$	Outgoing longwave radiation (W/m^2).
LE	Latent heat loss by evaporation (transpiration) (W/m^2).
M	Photochemical heat storage (W/m^2).
Q^*	Net radiation balance (W/m^2).
r_H	Resistance to sensible heat transfer (boundary layer) (s/m).
r_s	Stomatal resistance to water vapor transfer (s/m).
r_v	Total resistance to water vapor transfer (s/m).
t	Length of averaging period (s).
T_{as}	Air temperature in vicinity (airspace) of seedling (°C).
T_ℓ	Leaf (needle) temperature (°C).
u	Windspeed (m/s).
WU	Apparent water use calculated from LE (cm^3).
β	Bowen ratio; H/LE (unitless).
λ	Latent heat of vaporization (2450 J/g).
ρ	Density of air ($\sim$ 1200 g/m^3).
ρ^l	Saturated vapor density of needle at needle temperature (g/m^3).

ρ_a Air vapor density of seedling airspace (g/m^3).

ρ_w Density of water (1.0 g/cm^3).

Energy Exchange of Transplanted Douglas-fir Seedlings on Two Cutover Sites in Southwestern Oregon

INTRODUCTION

There is a history of reforestation failure on cutover sites in southwestern Oregon (Minore, 1978; Hobbs et al., 1979) and northern California (Strothmann, 1976). Heat and moisture stress have been implicated as the major causes of seedling mortality on many sites (Strothmann, 1976; Minore, 1978; Hobbs et al., 1979; Helgerson et al., 1982). In response to this reforestation failure, several techniques have been tried in an attempt to favorably modify the microclimate in a way to increase the survival of transplanted seedlings. Of these techniques, the use of shadecards and the shelterwood harvest system have been two of the most widely used and recommended (Minore, 1971; Ryker and Potter, 1970; Lewis et al., 1978; Minore, 1978; Williamson and Minore, 1978; Hobbs et al., 1979; Hobbs et al., 1980). The main objective of these two techniques is to reduce the heat loading upon the seedlings by blocking out incoming solar radiation. Although these methods are currently standard practices in reforestation of cutover lands in southwestern Oregon, their effectiveness has generally been proven only qualitatively, and not to any quantitative extent, by past research.

Strothmann (1972) found that natural shading had no effect on the survival of conifer seedlings on hot, dry slopes in northern California. Later, Strothmann (1976) tested four different planting treatments of Douglas-fir [Pseudotsuga menziesii (Mirb.) Franco] seedlings and found that all treatments had similar percentage

survival, stem shading included, after ten years. Hobbs et al. (1980) determined that shadecards improved 1-0 containerized seedling survival by 16% on south aspects, but that this was not significant at the $p = 0.05$ probability level. They, however, recommended using shadecards on south- and west-facing slopes. Helgerson et al. (1982) showed that shading significantly increased survival of natural regeneration of Douglas-fir and white fir [Abies concolor (Gord. & Glend.) Lindl.], but not that of transplanted Douglas-fir or ponderosa pine (Pinus ponderosa Dougl.). Instead, they suggest that shading may be unnecessary for transplanted nursery stock and that seedling quality was more important than microsite shading under a shelterwood canopy. Woodard (1966) advocated the use of shade after a study which showed that shade from shade frames postponed the death of potted Douglas-fir seedlings which lacked available soil moisture during hot, dry weather. Lewis et al. (1978) found that shadecard shading of 2-0 Douglas-fir seedlings increased survival on soils with low water-holding capacity, but not on soils with high water-holding capacity. They concluded that shading with cards was significant enough to advocate the continued use of the clearcut harvest system with shadecards as a reforestation tool, instead of using the shelterwood harvest system.

Little has been learned regarding the effectiveness of the residual canopy in a shelterwood harvest system upon reforestation success in southwestern Oregon. Williamson and Minore (1978) found that the presence, or absence, of an overstory canopy was the single most important factor in seedling survival in relation to frost and pocket gopher damage. Seidel and Cooley (1974) looked at the establishment

and survival of grand fir [Abies grandis (Dougl.) Lindl.] and mountain hemlock [Tsuga mertensiana (Bong.) Carr.] under a shelterwood cutting in the Oregon Cascades. They found that in the areas of higher stand density, more seedlings of both species were established, and that grand fir seedlings had a higher survival rate. Also, although the study of Helgerson et al. (1982) was under a shelterwood, the influence of shading by the trees making up the residual, shelterwood canopy was not considered.

OBJECTIVES

All of the previously mentioned field studies have attempted to determine the effectiveness of shade to seedling survival from a statistical characterization of the seedling response. The output from these large population studies is frequently of a binary (discontinuous) nature, i.e., dead or alive. Others use continuous variables like stem height growth or diameter growth as an indication of the effectiveness of the treatment upon seedling survival and/or growth. Standard statistical tests are then performed to determine whether these differences are significant. If a treatment proves to be statistically significant in terms of survival, then inferences are made in an attempt to explain how or why the treatment works. This type of approach is usually not able to identify or describe the causal relationships involved. Due to the many factors involved, and their large natural variability, only guesses can be made concerning the physical processes which control the microclimate of transplanted seedlings and, therefore, govern their establishment.

The major objective of this study was to apply an analytical tool, the energy balance, to this reforestation problem in an attempt to compare the relative effectiveness of shadecards to the shelterwood harvest system for ameliorating the microclimate of transplanted Douglas-fir seedlings. It involved monitoring those variables which describe the microclimate of the seedlings and their response. This was done by measurements of needle temperature and stomatal resistance. By making continuous measurements of the response variables and by normalizing them to allow between-seedling comparisons, much

of the variation which hinders analysis in other studies was reduced or eliminated. The objective, then, was to see if differences in the energy balance terms and water use can be detected and serve to interpret treatment effects. Since both kinds of treatments, shade-cards and the shelterwood harvest system, are assumed to act primarily to increase shade, this will also allow a comparison between the type of shade, i.e., a small area of influence versus a large area of influence. Because of the difficulty in assessing net radiation, a second objective involved comparing solar radiation calculated by a model simulating seedling geometry, solar radiation received by a sphere, and solar radiation measured by a horizontally-oriented radiometer. Also, the amount of water used by the seedlings over the summer season will be investigated, because of its importance in understanding the water stress phenomenon.

Energy Balance Theory

Energy balance studies have been used in the analysis of the thermal energy exchanges associated with many types of surfaces and organisms. The energy balance equation for an organism (Monteith, 1973) can be written:

$$Q^* + M - LE - H \pm J - G = 0 \qquad (1)$$

where Q^* is the net gain of energy from radiation (net radiation), M is the net gain of energy from metabolism, LE is the loss of latent heat by evaporation, H is loss of sensible heat by convection, J is the change in stored heat, and G is loss of heat by conduction into

the environment. For plants, M represents photochemical heat storage which is negative on balance and is small enough relative to Q* that it can be ignored (Monteith, 1973; Sinclair et al., 1975). The terms G and J have also been found to be small (Sinclair et al., 1975; Tanner and Lemon, 1962; Monteith, 1973) and will also not be considered in this study. For Douglas-fir seedlings, therefore, the energy balance can be rewritten as:

$$Q^* - LE - H = 0 \tag{2}$$

with LE and H (W/m^2 units) representing the predominant heat loss modes.

It is important to separate the energy source term, Q*, into its four components as:

$$Q^* = K\downarrow - K\uparrow + L\downarrow - L\uparrow \tag{3}$$

where K↓ is the incoming shortwave (solar) radiation, K↑ is the outgoing solar radiation, L↓ is the incoming longwave radiation, and L↑ is the outgoing longwave radiation.

The latent heat flux term, LE, in equation 2 is described by:

$$LE = \lambda \frac{\rho^l - \rho_a}{r_v} \tag{4}$$

where LE is the flux in watts per square meter (W/m^2), ρ^l is the saturated vapor density of the needle at the needle temperature (g/m^3), ρ_a is the vapor density of the airspace around the seedling

(g/m^3), r_v is the resistance to the flow of water vapor from the leaf to the air (s/m), and λ is the latent heat of vaporization for water (2450 J/g). The water vapor resistance, r_v, is made up of three resistance terms representing the intercellular air space, stomata, and boundary layer on the leaf surface (Nobel, 1974). The first two resistances can be measured by the null balance diffusion method (Beardsell et al., 1972) and those two combined are generally larger than the boundary layer resistance except when stomatal resistance is very low (Nobel, 1974). Therefore, r_v in equation 4 can be replaced by r_s, the stomatal-intercellular air space resistance (commonly designated as stomatal resistance).

The sensible heat flux term, H, in equation 2 is described by:

$$H = \rho C_p \frac{T_\ell - T_a}{r_H} \qquad (5)$$

where H is the flux in W/m^2, ρ is the density of air, C_p is the specific heat of air (1.01 J/g °C), T_ℓ is the leaf (needle) temperature (°C), T_a is the seedling airspace temperature, and r_H is the resistance to thermal transfer, the boundary layer resistance. This resistance can be calculated by:

$$r_H = 307(d/u)^{1/2} \qquad (6)$$

where r_H is in units of s/m, d is the characteristic dimension of the needles, the diameter in this case, in units of m, and u is the windspeed in m/s (Campbell, 1977). Equation 6 gives the resistance to heat transfer from one side of a flat plate and was determined by heat

transfer theory (Campbell, 1977). It has been suggested (Campbell, 1977) and shown (Fritschen et al., 1980) to be a useful relationship for the evaluation of r_H for cylinders, the geometric analog of a conifer needle.

The ratio of the sensible heat flux to the latent heat flux is called the Bowen ratio and is represented by:

$$\beta = H/LE \tag{7}$$

where β is the Bowen ratio. It is a measure of the partitioning of heat exchange by the two processes. Because it is independent of Q^*, β allows a comparison between various objects or surfaces which are under different radiation regimes. If $\beta > 1$, most of the heat energy is being dissipated as H, and if $\beta < 1$, most of the heat is being dissipated as LE through the evaporation of water. If β is negative, the two modes are of different sign and one of the fluxes is towards the surface or object. This can occur when dew is forming (condensation) or in an advective situation, when sensible heat from a surrounding dry area is used to evaporate water from a surface such as a lake, or from vegetation. Examples of this are grass lawns (Oke, 1979) and shade trees (Halverson and Potts, 1981) in urban areas, and marshes in deserts (Gay and Holbo, 1971). Oke (1978) listed average daily values of β of 0.4 to 0.8 for temperate forests, 2.0 to 6.0 for semi-arid areas, and 10.0 for deserts. Thus, negative values are apparently rare for natural surface covers. For coniferous canopies, daily values of β have been measured as 1.67 for Scots pine (Pinus sylvestris L.) and Corsican pine (Pinus spp.) in England, 0.70 for

Douglas-fir in Washington (Gay and Stewart, 1974) and 0.48 for Douglas-fir in British Columbia (McNaughton and Black, 1973). Moore (1976) measured β over a Pinus radiata canopy with eddy-correlation equipment and found that $\beta = 0.8 \pm 0.1$ for a day when the canopy was dry and $\beta < 0.3$ when the canopy was wet. Murphy et al. (1981) found that β ranged up to 2.3 over a loblolly pine (Pinus taeda L.) canopy in April and May. Reported Bowen ratios for individual plants are much fewer in number. Fritschen et al. (1980) worked with an isolated Scots pine and calculated daily values of β ranging from 2.8 to 17.0 for 4 days in August and September.

The Study Sites

The study sites were located at an elevation of 1310 m (4300 ft) on the Cave Creek drainage of the Siskiyou National Forest in southwestern Oregon (SW1/4, NE1/4, Sec. 4, T. 40 S., R. 6 W.). The sites are approximately 2 miles northeast of the Oregon Caves National Monument and 12 miles east of the town of Cave Junction, Oregon.

The study was performed on two cutover sites, a 17-acre clearcut and a 52-acre partial-cut (shelterwood) that were located beside each other. The clearcut had a southerly aspect and an average slope of 40%. The partial-cut had a southwesterly aspect and an average slope of 25%. The clearcut had been harvested in 1965 and broadcast burned in 1967. Four previous attempts at reforestation were unsuccessful. The site contains some scattered small Douglas-fir and ponderosa pine and numerous clumps of snowbrush (Ceanothus velutinus Dougl.). Other major plants indigenous to the site are green-leaf manzanita (Arctostaphylos patula Greene), senecio (Senecio spp.), blackberry

(Rubus spp.), and assorted perennial grasses. The partial-cut was harvested in 1979 and the post-harvest slash broadcast burned in 1980. The residual canopy, about 27% of the original basal area, is made up of Douglas-fir, ponderosa pine, white fir, sugar pine (Pinus lambertiana Dougl.) and incense-cedar [Libocedrus decurrens (Torr.) Florin.]. Major understory vegetation at present is Russian thistle (Salsola kali L.) and assorted perennial grasses. The soil on both sites is a gravelly sandy loam derived from granodiorite and gabbro bedrock (Karen Jones, U.S. Forest Service, personal communication).

Two small plots, one on each site, were established in which to plant seedlings for the 1981 study. Planting locations in the clear-cut were sprayed in the Autumn of 1980 with 2% solution of glyphosate (Monsanto Co.; tradename: Roundup) in an attempt to limit weed competition the following spring. Planting locations in the partial-cut were scalped manually to a diameter of 1 m in February, 1981, immediately before seedlings were planted.

Sixty-four 2-year-old (2-0) bareroot seedlings were planted in each plot on a 3 x 3 m spacing in auger holes in February, 1981. The auger made a hole of 15 to 20 cm diameter and approximately 30 cm deep. The seedlings planted were selected from a group of 200 seedlings from the U.S. Forest Service nursery in Medford, Oregon. The seed for these seedlings were collected in 1971 from the 1370 m (4500 ft) elevation level in what was regarded as the appropriate seed zone for the Cave Creek site (Karen Jones, personal communication). A conventional 30 x 20 cm shadecard was placed 10 cm from the stem on the southwest side of half of the seedlings planted per site.

For energy balance measurements, a pair of seedlings on each plot were chosen so as to match each other in size and microsite characteristics as closely as possible. One of each seedling pair had a shadecard beside it. The four seedlings, therefore, represented four treatments: clearcut/no card (CN), clearcut/shadecard (CS), partial-cut/no card (PN), and partial-cut/shadecard (PS). This way, the energy balances of the seedlings influenced by the shelterwood harvest system and by shadecards could then be compared in relation to the success of the treatments in ameliorating the microclimate of the seedlings.

Site Data

Meteorological stations on each site recorded air temperature, dewpoint temperature, incoming solar radiation ($K\downarrow$), and windspeed at a level 2 meters above ground surface, dewpoint temperature at approximate seedling height (20 cm), photosynthetically-active radiation (PAR) and precipitation at the ground surface.

Air temperature was measured with a thermistor (YSI Co.; Yellow Springs, Ohio; part no. YSI 44202) in a half-bridge network. The thermistor was mounted within a radiation shield which was designed and painted to minimize radiative heat transfer to the thermistor. Dewpoint temperatures were measured with a dewcel-type hygrometer (Holbo, 1981) using lithium chloride as the humidity-sensing element. These units were also shielded from solar radiation. Incoming solar radiation was measured with a Moll-Gorczynski pyranometer (Kipp & Zonen; Delft, Netherlands). Windspeed was measured with a 3-cup contact-closure anemometer (Met One, Inc.; Grants Pass, Oregon).

Photosynthetically-active radiation (PAR), that portion of the solar spectrum between 0.4 and 0.7 μm wavelength, was measured with a spherical sensor (Li-Cor, Inc.; Lincoln, Nebraska; model LI-193SB) that is uniformly sensitive to radiation, regardless of its angle of incidence. Precipitation was measured in a tipping bucket rain gauge (Texas Electronics, Inc.; Dallas, Texas; model 525) which gave a pulse signal for every 0.01 in (0.25 mm) of precipitation collected.

All signals from the meteorological station instruments were sampled at 0.1 Hz and logged by a microprocessor-controlled datalogger (Campbell Scientific, Inc.; Logan, Utah; model CR-21). The datalogger summed the precipitation signal and averaged the other signals over 30-minute periods and stored the digital output on a cassette tape. The meteorological stations collected data continuously throughout the summer of 1981 at the two cutover sites.

In addition to the energy balance study, a study of soil temperatures on the two sites was being conducted at the same time (Childs et al., 198X). For this study, soil temperatures were measured at 5 depths (2, 4, 8, 16, and 32 cm below soil surface) by a probe consisting of 5 thermistors (YSI Co.; Yellow Springs, Ohio; part no. YSI 44202). Further details of the instrumentation are described by Holbo et al. (198X). Ten probes were deployed beside five seedlings on each site. Five of the probes were on the northeast side of a seedling and five were on the southwest side of a seedling. These measured soil temperature profiles were used to make estimates of the soil surface temperature for calculating longwave flux to the seedlings.

Seedling Response Data

The measurements chosen to characterize the seedling response were needle temperature and stomatal resistance. The temperature of a seedling's needles, and its divergence from air temperature, represent the degree to which the seedling is in thermal equilibrium with its surroundings. Needle temperature also represents the only measurement which allows a continuous monitoring of seedling response. Stomatal resistance is also an important variable, but it can not be measured on a continuous basis due to the requirement for placing the tissue in a cuvette and, ultimately, for removal of the tissue so that needle area can be determined.

Needle temperatures were measured with 0.05-mm (0.002-in) copper-constantan thermocouples (Omega Engineering, Inc.; Stamford, Connecticut) looped around individual needles with the junction tightened against the bottom of the needle. A small drop of white heatsink compound insured good thermal contact between the thermocouple junction and the needle. Visual observation revealed no physiological damage to the needles from the compound even after several months. From two to four, generally three, were connected in parallel and referenced to another thermocouple which was allowed to hang in the air beside the tree. This arrangement provided a voltage signal proportional to a 2-, 3-, or 4-needle average of the leaf-to-air temperature difference, dT. In addition, the air thermocouple was separately referenced to a bridge-type junction simulating 0°C (Omega Engineering, Inc.; Stamford, Connecticut; model LXCJ-T). This arrangement gave the actual value of the air temperature, T_{as},

immediately beside the tree (referred to hereafter as airspace temperature to distinguish it from the air temperature measured at the 2-m level). The dT voltage signal was amplified by 200, which obtained a temperature resolution of 0.012°C and an accuracy within $\pm$ 0.01°C. The voltage signal for airspace temperature was amplified by 50, which obtained a resolution of 0.05°C and established an accuracy within $\pm$ 1.0°C. The signals were logged on a digital datalogger (Campbell Scientific, Inc.; Logan, Utah; model CR-5) by way of a rapid-sampling integrator module (2.4 Hz) such that the recorded data represented 15-minute averages of the measured variables (dT, T_{as}).

Because stomatal resistance measurements require destructive sampling, they were not made on the four seedlings chosen for the energy balance study. Instead, seedlings in the immediate area were used. This allowed a characterization of the stomatal resistance pattern for seedlings with and without shadecards. Stomatal resistance was measured by the null balance diffusion method (Beardsell et al., 1972) using a null balance porometer (Interface Instrument; Corvallis, Oregon). During each site visit, a series of measurements, at approximately hourly intervals, were made on 6 or 7 seedlings per site. The branch portions used were clipped at the end of the day-long run and frozen to maintain the tissue moisture content. The leaf area was measured later in the laboratory with a leaf area index meter (Li-Cor, Inc.; Lincoln, Nebraska; model LI-3000). Leaf temperature and stomatal resistance were measured on previous-year foliage in May, and upon the current-year foliage in July and August.

The four needle-temperature seedlings were dug up, potted, and brought back to the laboratory in late August. Seedling orientation

in the field was noted and duplicated in the laboratory. The geometrical structure of each seedling was measured using the methods described in Appendix A. Measurements included vertical and horizontal angles, and total leaf area of each branch. This information was used in the program SEEDRAD (Appendix B), along with the relationships for the solar geometry (longwave view factors, measured site K↓) to calculate the various fluxes given by Equation 3. Thus, the net radiation flux density was determined at half-hour intervals through the day for each seedling.

Needle temperature, soil temperature, and stomatal resistance were measured during the periods May 20-June 1, June 15-18, July 2-5, August 5-9, and August 24-28. During these visits, soil temperatures were measured on both sites every day and at least one day-long set of stomatal resistance measurements were made. Needle temperature, however, could be measured at only one site at a time because only one set of junction boxes and amplifiers was available. The instrumentation, therefore, was alternated between sites during each visit. From this group of days, four days of cloudless sky conditions were chosen for seedling energy balance analysis. Days selected for the clearcut site were May 28, July 4, August 7, and August 27. For the partial-cut site, May 22, July 3, August 7, and August 27 were chosen. Unfortunately, not all days had a complete set of measurements so that some shifting of data had to be done. For example, stomatal resistance measurements made May 23 on the partial-cut were used on May 22 so as to line up with needle temperature and meteorological station (site) measurements. A schedule of the days from which measurements were taken is given in Table 1. Undoubtedly, some

unknown amount of error will result from this. The error is probably small, however, for stomatal resistance and needle temperature patterns on two or three sequential days of cloudless skies.

The breaking of buds, elongation of new tissue, and late-summer needle drop presented somewhat of a problem in the determination of leaf areas. Because the leaf area measurements were not made until September, estimates had to be made for the leaf areas present in May and July. This was done by distinguishing beween old (previous-year) and new (current-year) needles when calculating leaf area. Because very little elongation of new tissue had occurred at the time of the May measurements, the old-needle leaf area was used for May. Since needle drop of old needles occurred between the July and August site visits, estimates had to be made for July. One of the seedlings, PN, had almost all of its leaf area intact by late August, and it was used to estimate the amount of leaf area dropped by the other three seedlings between July and August. The leaf areas used for the four seedlings on the four days chosen are shown in Table 2.

Table 1. Schedule of measurements for leaf temperture (T_ℓ), stomatal resistance (r_S), and site variables used in energy balance calculations. May 22, JD 142; July 2, JD 183; August 5, JD 217; and August 25, JD 237.

Julian Date	CC			PC		
	T_ℓ	r_S	Site	T_ℓ	r_S	Site
142				X		X
143					X	
148	X	X	X			
183				X		
184						X
185	X	X	X		X	
217				X		
218		X			X	
219	X		X			X
220				X		
237		X			X	
238				X		
239	X		X			X

Table 2. Total leaf area (cm^2) of the four seedlings for each of four site visits. Treatment abbreviations are: C = clearcut, P = partial-cut, N = no card, and S = shadecard.

Seedling	May	July	Early August	Late August
CN	280	697	520	520
CS	405	970	684	684
PN	354	729	729	729
PS	371	851	782	782

METHODS

The first task in this study was to determine how to estimate the values for the energy fluxes given by equation 3 for each of the four seedlings. Since direct measurements cannot be made of the fluxes to and from a Douglas-fir seedling, a model of radiation geometry representative of the seedlings had to be used with site measurements of K↓ in order to calculate the solar flux (K↓) to the seedlings.

Several studies have been made of the interception of solar radiation by coniferous canopies (Norman and Jarvis, 1976; Gay and Stewart, 1974) and by individual trees (Mann et al., 1979; Fritschen et al., 1980; Ungs, 1981). Simulations of light interception by canopies usually deal with a form or modification of Beer's Law, which describes the passage of light through a homogenous medium. Because a seedling is a discrete object in three dimensions, such a two-dimensional model designed for canopies may be inappropriate. Models of light interception by individual plants usually assume some uniform geometric shape, such as a cone (Fritschen et al., 1980; Ungs, 1981) or an ellipsoid (Mann et al., 1979). It is possible that 2-year-old Douglas-fir seedlings are not well described by such models, and the error in assuming that the receiving surface of a seedling is represented by a cone or ellipsoid could be large. Consequently, a model was developed for this study which allows the calculation of solar radiation (K↓) to the seedlings. This model, called SEEDRAD, is described and documented in Appendices A and B. The model also calculates outgoing solar and incoming and outgoing longwave radiation flux densities for the seedlings and determines the net radiation (Q*) from

a summation of these fluxes. Comparisons between the model calculation of incoming solar radiation (K↓) and that received by a sphere and by a horizontal surface were also made to examine what geometric shape would best represent a Douglas-fir seedling.

Values of Q* from the program SEEDRAD (Appendix B) were used along with stomatal resistance patterns, leaf, airspace, and dewpoint temperatures in the calculations of H, LE, and β by the program HEATDUMP (Appendix C). Values for H were calculated by two different methods. Equation 5 was used with r_H calculated by equation 6. The other method was to calculate H as a residual in equation 2: Q* - LE.

RESULTS AND DISCUSSION

Site measurements of incoming solar radiation and the SEEDRAD model were used to calculate incoming solar radiation ($K\downarrow$ in watts per square meter) to each of the four seedlings. A set of typical patterns is shown in Figure 1 for August 7, 1981. Seedling CN, the only one without some type of shade, shows a very rapid increase in the morning and decrease in the evening with a somewhat flat peak in between. Seedling CS shows the same rapid increase in the morning as did CN, but a gradual decline begins at 1200 when the shadecard becomes effective. Integrating under the curves in Figure 1 shows that the daily value of $K\downarrow$ for CS (8.9 MJ/m^2) is 78% of the daily value of $K\downarrow$ for CN (11.4 MJ/m^2). The shadecard, therefore, decreased $K\downarrow$ by 22%.

The seedlings in the partial-cut show very large variations in the incident shortwave radiation. Seedling PN shows greater variation in the afternoon than in the morning. This is probably due to more tree stems in the southwest portion of the canopy, whereas some radiation is transmitted through the crowns to the southeast. Seedling PS shows the least amount of shortwave radiation as a result of both canopy and shadecard effects. The daily value of $K\downarrow$ for PN (8.1 MJ/m^2) and PS (6.0 MJ/m^2) are 71% and 53% of the value for CN (11.4 MJ/m^2), respectively. The partial-cut, therefore, decreased $K\downarrow$ by 29%, while the shadecard and partial-cut together decreased $K\downarrow$ by 47%. Comparing CS and PN shows that the partial-cut alone reduced $K\downarrow$ slightly more than that of the shadecard alone.

The incident shortwave radiation patterns for the seedlings in the partial-cut show many dips to as low as 70 W/m^2 at 1230 for both

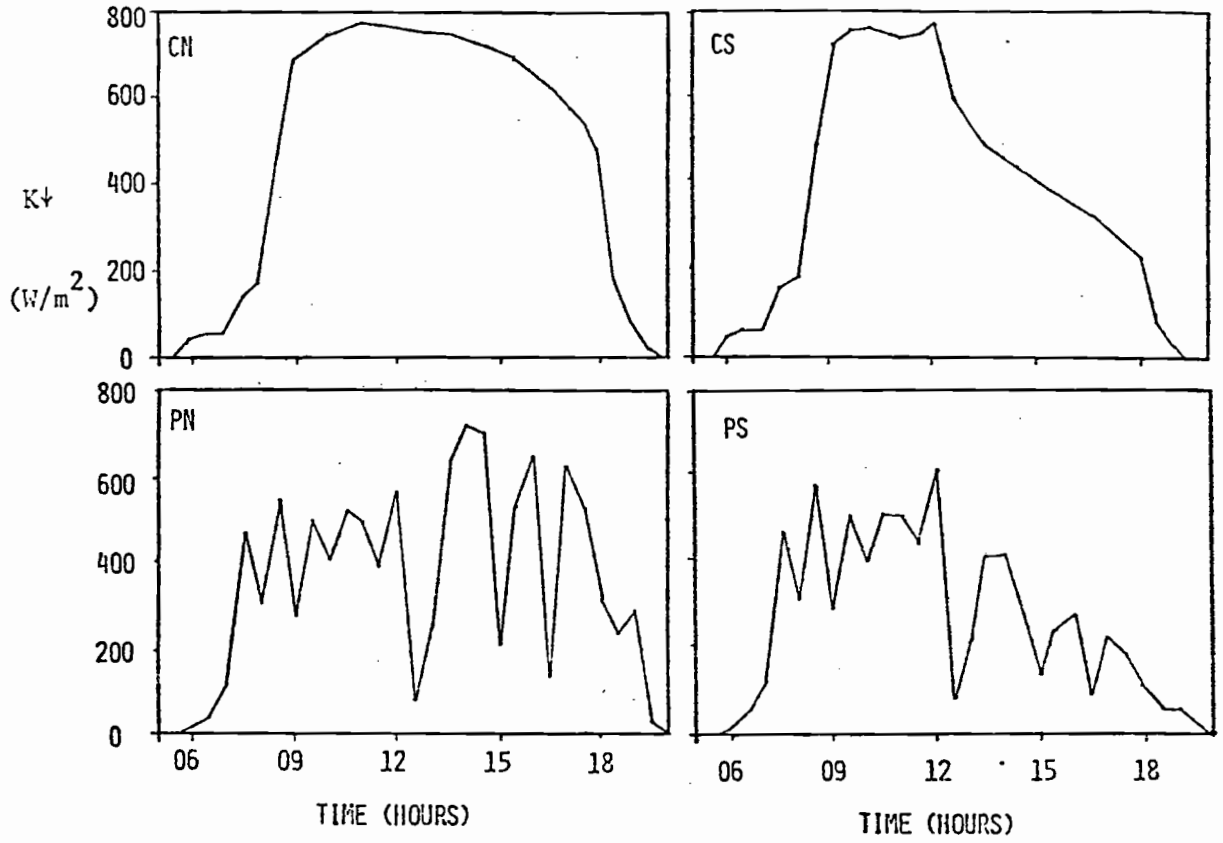

Figure 1. Incoming solar radiation (K↓) to Douglas-fir seedlings on August 7, 1981.

PN and PS. These shade events, because they cover a large volume of air, soil, and plant canopy, are postulated to have very important contributions to lowering the canopy-level air temperatures and, therefore, airspace temperature of the seedlings. Indeed, the air temperature at the 2-m level was approximately 2°C cooler throughout the mid-day period in the partial-cut than in the clearcut for this day (August 7) (unpublished data). This lower air temperature level will lower the vapor density deficit, a water demand variable (Tan and Black, 1976), for a given value of the needle-airspace temperature difference (dT). It is expected that a shadecard will not produce a similar effect due to the small soil-plant-air volume which it influences.

Comparison Between Geometrical Shapes

The shape of the K↓ curve for CN is compared with that of two uniform geometrical shapes in Figure 2. These are normalized by the maximum half-hour value of K↓ so that the ordinate represents fractions of the maximum value. The shape of K↓ for CN, developed from the SEEDRAD model and site measurements, compares more favorably with the incoming radiation to the spherical PAR sensor than with that of a flat surface as represented by the horizontally-oriented pyranometer. The agreement between the seedling and the spherical PAR sensor is probably sufficient to allow either the model representation of a seedling as a sphere, or the use of a spherical PAR sensor for quantifying incident radiation to Douglas-fir seedlings. Figure 2 also shows the error in trying to measure the solar radiation received by an isolated plant with a horizontally oriented pyranometer. The use

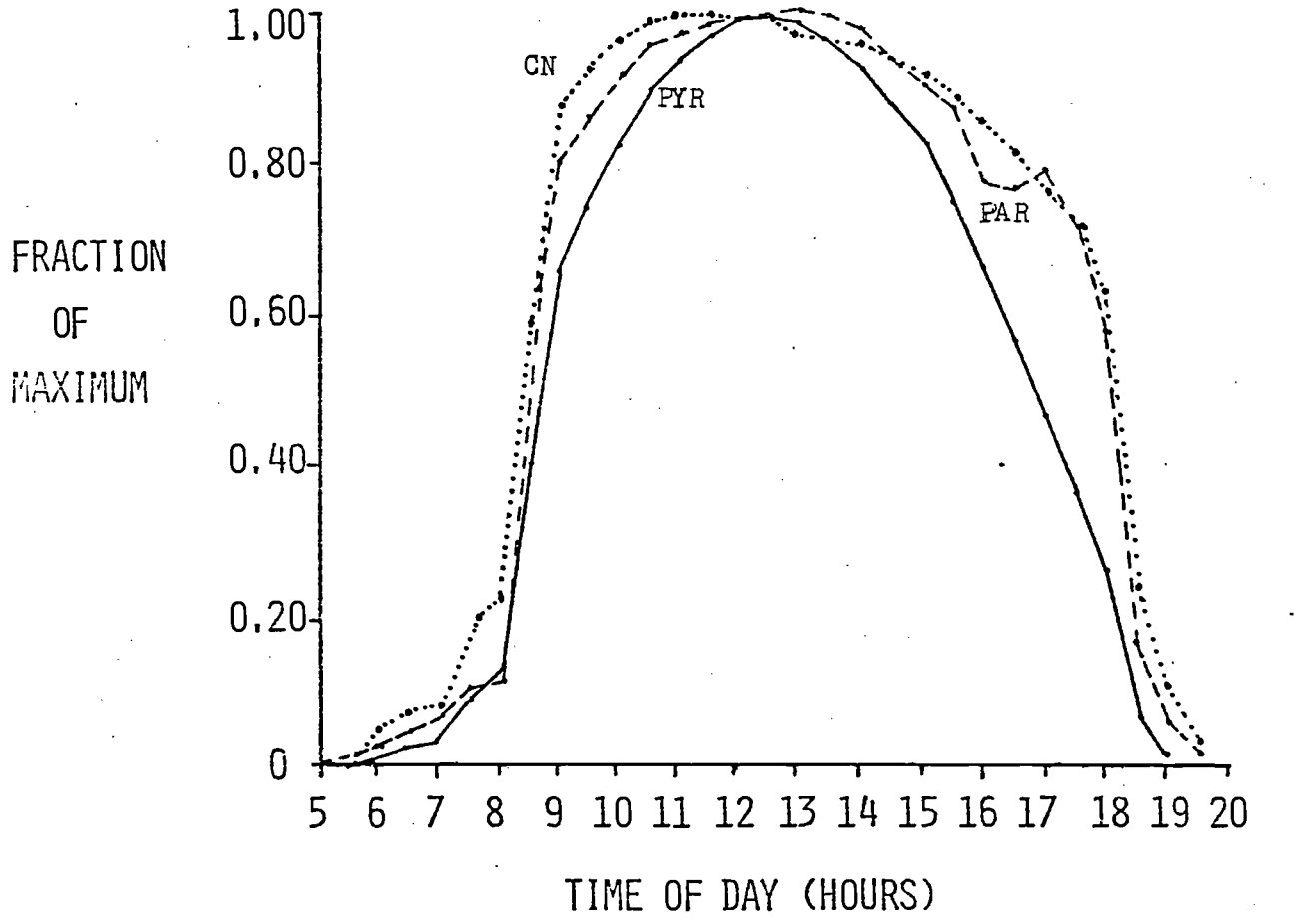

Figure 2. Incoming solar radiation ($K\downarrow$) normalized to maximum half-hour value for a Douglas-fir seedling (CN), a spherical PAR sensor (PAR), and a horizontally-oriented pyranometer (PYR) for data collected August 7, 1981.

of flat-plate radiometers, which measure Q*, has also been deemed inappropriate for measuring net radiation to isolated trees (Fritschen et al., 1980).

Partitioning of Net Radiation

Net radiation values from the program SEEDRAD were used in the program HEATDUMP, along with seedling response and site measurements to partition net radiation (Q*) into convective (sensible) heat exchange, H, and into latent heat exchange, LE. Equation 4, along with measurements of the leaf-to-air vapor density deficit and stomatal resistance, was used to calculate values for LE. Two methods were used to calculate the sensible heat flux, H, from the seedlings. Equation 6 was used with the approximation that u = 0.3 x (2-m windspeed) and d = 1 mm in order to calculate r_H. The seedling-level windspeed was found to be an average fraction of 30% of the 2-m windspeed from several windspeed profiles measured in the summer of 1981 (Vanderwaal, unpublished data). Measured values of $T_\ell - T_{as}$ and calculated values of r_H were then used in equation 5 to calculate H. The alternate method was simply to calculate H by difference: $H = Q^* - LE$.

Calculated values of H were far less than the value of H by difference. For example, on August 7, 1981, the mean daily value of H for seedling CN was 77.9 W/m^2 and 187.0 W/m^2 as calculated by equation 5 and by difference, respectively. Equation 5 underestimated the H required to balance the energy balance by 58%. When individual half-hour means were considered, the underestimation was even greater. For

example, at 1500 on August 7, the equation 5 calculation of H was only 1% (5.3 of 515 W/m^2) of the value of H by difference. The use of equation 5, therefore, was considered unjustified for this study. Since $T_{\sim} - T_{as}$ measurements were fairly accurate ($\pm$ 0.1°C), the large errors in using equation 5 were probably a result of the errors in determining r_H by equation 6. Since Fritschen et al. (1980) had fairly good success with equations 5 and 6 in determining H for an isolated Scots pine (Pinus sylvestris), the difficulty probably lies with the measurement, or calculation, of the windspeeds occurring at the level of the seedlings. The value of H, therefore, was taken as the value by difference, since this method provides a balance in the energy balance equation (i.e., $Q^* - LE - H = 0$).

Figure 3 shows the results of May 28 and August 7 for seedling CN as an example of the partitioning of net radiation. As evident in the figure, the net radiation, Q*, has a shape similar to that of the incident shortwave ($K\downarrow$) seen in Figure 1 (CN). Radiation studies over Douglas-fir forest canopies (Gay and Stewart, 1974) have shown a similar pattern, and it does make sense, since $K\downarrow$ is the largest component in Q*. It is also evident that the majority of Q* is dissipated as H, rather than as LE. Fritschen et al. (1980) found this also to be typical for an isolated Scots pine. Whole forest canopies, however, do not show this large value of H and this will be discussed later when considering the Bowen ratio. Figure 3 also shows a slight increase in H and a corresponding decrease in LE between May 28 and August 7. This is mainly due to a decrease in water use, and thus, LE, by seedling CN, rather than an increase in the convective heat dissipation, H.

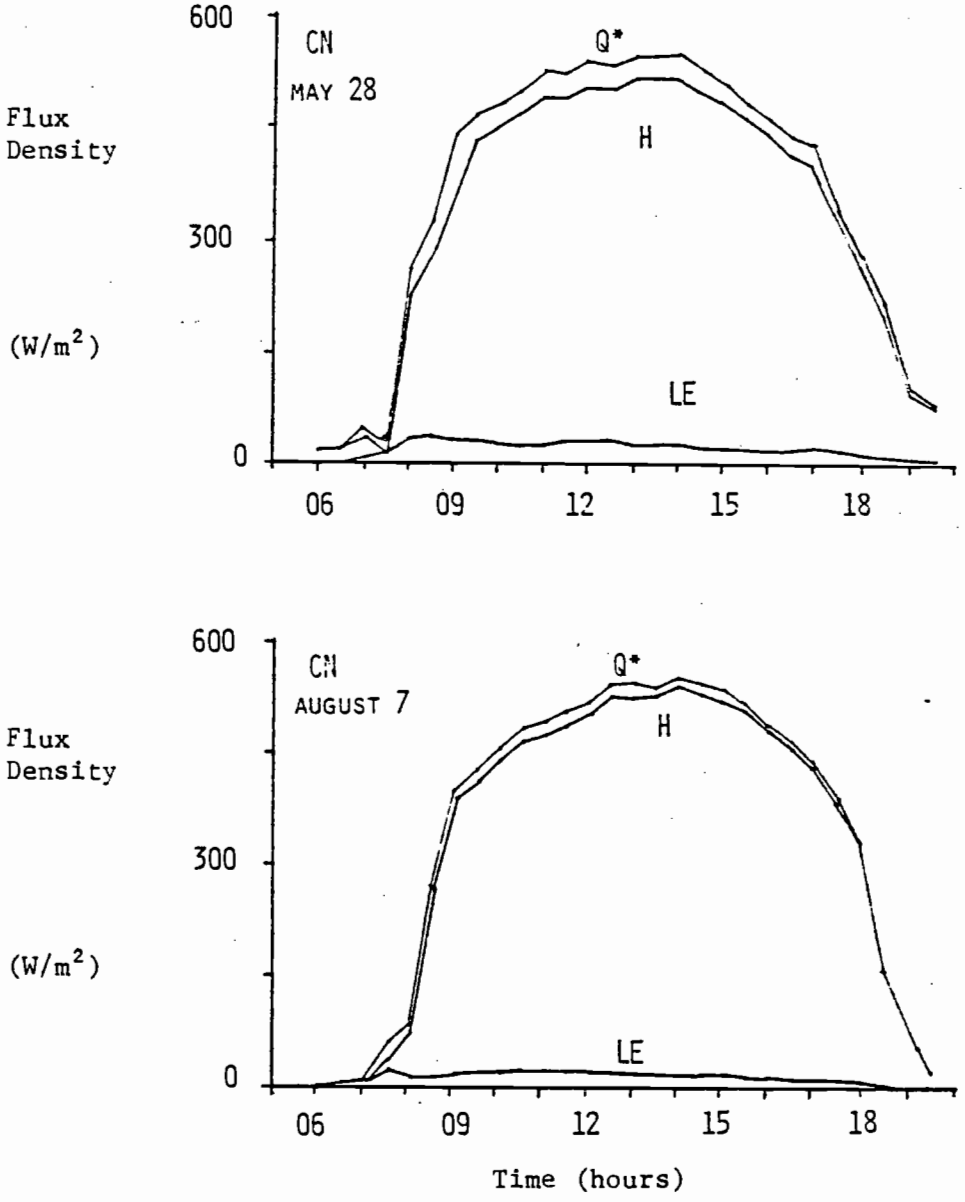

Figure 3. Net radiation (Q*) partitioning into sensible heat flux (H) and latent heat flux (LE) for seedling CN on May 28, 1981, and August 7, 1981.

Values of Q*, H, LE, and β, the Bowen ratio, are shown in Table 3 for all seedlings on the four selected days from the summer of 1981. These data represent the daily average of each flux in W/m^2. The Bowen ratio, β, is determined by H/LE (which is actually (Q* - LE)/LE in this study), and represents the relative partitioning of Q* between the modes of heat exchange. Values of Q* can not be compared between the two sites directly for the May and July days due to differences in incoming solar radiation from partial cloud cover occurring on May 22 (partial-cut) and July 4 (clearcut). It is interesting to note that on August 27 the Q* was greater for PN than for CS. This could result from a higher longwave input to PN than CS but, more likely, results from the sun track being lower in the sky. This would put the sun track through the stem area of the view of PN rather than in the crown area where there is a greater amount of vegetative material for shading. A lower sun track would also make the shade card beside CS effective more of the time.

Error in Energy Balance Measurements

Since all of the energy balance terms represent indirect measurements that are functions of more directly measured quantities, an analytical framework was required to estimate the error in the derived terms. A method presented by Scarborough (1966) was used since it has proved to be both easy to perform and effective in previous studies (Holbo, 1973; Sinclair, 1972; Sinclair et al., 1975). The theory is presented briefly and the error in the energy balance terms are calculated in Appendix D. The resulting probable error of each of the derived energy balance terms are shown in Table 4.

Table 3. Mean daily half-hour values of net radiation (Q*), sensible heat flux (H), latent heat flux (LE), and the Bowen ratio (β) for all four seedlings on the four selected days in the summer of 1981.

Seedling	Q*	H	LE	β
		W/m^2		
		May 21, 28		
CN	204	-191	-13	14.7
CS	149	-132	-17	7.8
PN	83	- 73	-10	7.3
PS	61	- 52	- 9	5.8
		July 3, 4		
CN	149	-140	- 9	15.6
CS	122	-115	- 7	16.4
PN	175	-161	-14	11.5
PS	143	-127	-16	7.9
		August 7		
CN	193	-187	- 6	31.2
CS	151	-146	- 5	29.2
PN	145	-126	-19	6.6
PS	103	- 91	-12	7.6
		August 27		
CN	193	-190	- 3	63.3
CS	133	-130	- 3	43.3
PN	156	-146	-10	14.6
PS	106	- 96	-10	9.6

Table 4. Relative probable error in the energy balance terms.

Q*	LE	H	G
2%	15%	3% (2 to 6%)	16% (15 to 20%)

An objective analysis, as provided by a framework such as Scarborough's, also allows for the determination of the variable, or measurement, which makes up the largest part of the final error. The results from the calculations (Table 4 and Appendix D) show that LE had the greatest amount of error in its calculation. Although a value of 15% seems high, it is in the same range as that found by other micrometeorological studies. For example, Holbo (1973) reported average errors of 25% and 30%, respectively, for aerodynamic model and Bowen ratio model estimates of LE. Indeed, many of the studies reviewed did not have any type of error analysis, or else the standard deviation of the measurements was used. While the standard deviation statistic is valid, it relates only to the precision of the measurements around the means and does not describe the accuracy of those measurements. An analysis, such as that presented by Scarborough (1966), allows an estimate of the probable error that could be expected and gives an estimate of the accuracy of the derived energy balance terms.

Within the computation of LE, there are three measurements whose errors add to give the error in LE. Of these three measurements, stomatal resistance makes up the largest portion, about 95%, of the total error in LE. An improvement in the instrumentation and methods used to make stomatal resistance measurements, therefore, would cause a large decrease in the error in LE. The other two measurements, leaf temperature and dewpoint temperature, combined to make up only about 5% of the error in LE. If the accuracy of these temperature measurements ($\pm$ 1°C) could be improved, or if the vapor density deficit, which these temperatures were used to calculate, could be measured more accurately, another, smaller, reduction in the error in LE could be attained.

Although the Bowen ratio, β, also had a large error (Table 3), this was a result of the way in which β was calculated for this study (i.e., $\beta = (Q^* - LE)/LE$). If β could have been calculated by H/LE, where H is a result of measurements rather than by difference ($Q^* - LE$), the error in β might have been smaller.

Bowen Ratios

Bowen ratios allow a direct comparison among seedlings and days. Table 1 shows the mean daily Bowen ratios for each seedling and Figure 4 shows the trend in β for the summer of 1981. The Bowen ratio increases greatly throughout the summer period for the two seedlings in the clearcut (CN and CS) but shows only a slight increase for the two seedlings in the partial-cut (PN and PS). An important point to notice is that there is a great difference between sites, especially in August, and very little difference between seedlings on a site. In

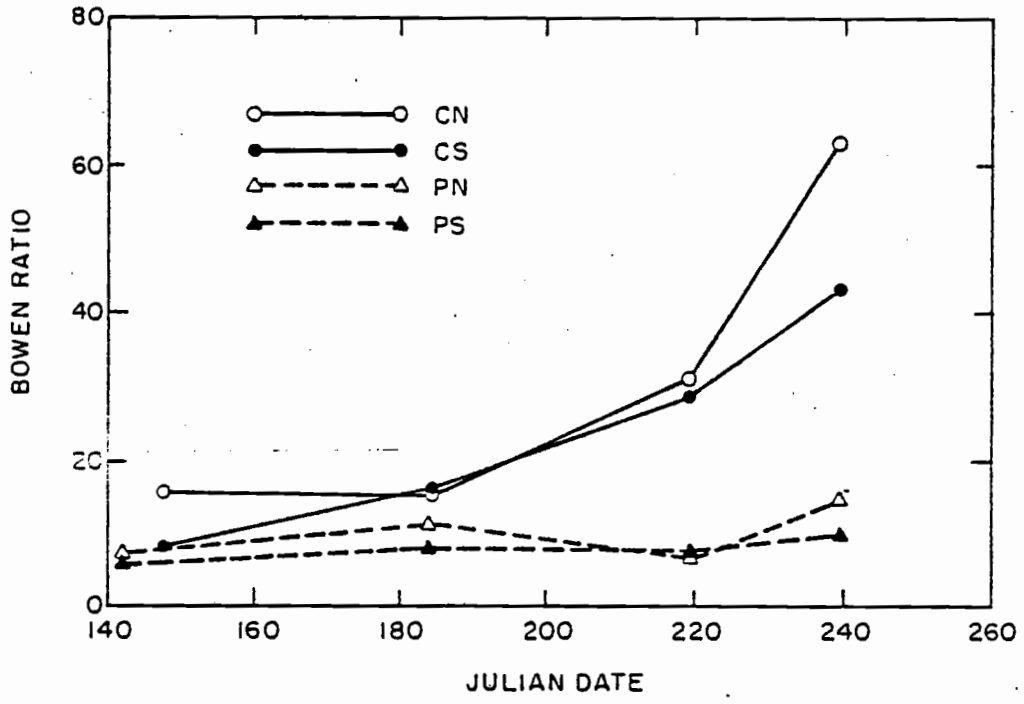

Figure 4. Seasonal trend in the Bowen ratio for four Douglas-fir seedlings on two cutover sites in southwest Oregon in the summer of 1981. (C = clearcut, P = partial-cut N = no card, and S = shadecard.)

other words, there appears to be a greater difference in comparing between the clearcut and partial-cut than in either of the shade card/no card comparisons.

The mean daily Bowen ratios ranged from a low of 5.8 (PS on May 22) to a high of 63.3 (CN on August 27). These numbers compare very well with the only other set found for a single conifer tree, that of a Scots pine in Washington (Fritschen et al., 1980). The Bowen ratios for this tree ranged from 2.8 to 17.0 for 4 days in August and September. The seedlings' values of β are quite large, however, when compared to those measured over coniferous forest canopies. For example, Jarvis et al. (1976) reviewed 19 studies performed over coniferous canopies and found that β ranged from 0.1 to 10 for dry canopies on sunny days and from -0.7 to 2.1 on overcast days. The average value is more on the order of 0.4 to 0.8 (Oke, 1978). This discrepancy has also been found between β values of leaves and whole canopies for deciduous trees (Knoerr and Gay, 1965; Knoerr, 1967). The reason is that the β of a canopy is an integration over all of the leaves (needles) of the canopy, from those in the top which are fully exposed to solar radiation, to those near the bottom which are shaded from solar radiation. The leaves near the top of the canopies have been found to have leaf temperatures well above air temperature so that most of the heat is dissipated by convection (Gates, 1963; Knoerr and Gay, 1965; Miller, 1967). In contrast, the leaves near the bottom often have leaf temperatures below air temperature (Gates, 1963; Miller, 1967) and, therefore, often gain heat from convection. In this situation, all of the heat loss occurs as latent heat (transpiration) and resultant β values are low or even negative

(Knoerr, 1967). Thus, the seedlings, with nearly all of their needles exposed to solar radiation, would be expected to have high β values with the majority of Q* being partitioned into H.

Diurnal Patterns of β and LE (Water Use)

The effect of the shade card upon the Bowen ratio is shown in the diurnal patterns for August 7, 1981 (Figures 5 and 6). The Bowen ratio for CS (Figure 5) is higher than for CN all morning but drops sharply at 1200 when the shade card first becomes effective. In the afternoon, β for CS is relatively constant while β for CN increases steadily. This produces a great difference between the two ratios. The shade card effect is less dramatic in the partial-cut (Figure 6). The Bowen ratio for PS, higher than for PN in the morning, also drops at 1200 when the shade card beside it becomes effective. The effect of the card on PS in the afternoon appears to be mainly that of a decrease in the fluctuation, or peaks, in β.

It is fairly evident that a shade card reduces the net radiation of a seedling, but a reduction in β, which occurred with the above two seedlings (CS and PS), means that there is also a change in the partitioning of the heat loss. A decrease in β can be caused by either a decrease in H, an increase in LE, or both. Figures 7 and 8 show the diurnal patterns of water use (a measure proportional to LE) for the seedlings on August 7, 1981. LE is converted to water use by $WU = LE(t)A/\lambda\rho_w$, where A is the total needle surface area, t is the length of the averaging period (30 minutes in this case), λ is the latent heat of vaporization (2450 J/g), and ρ_w is the density of water

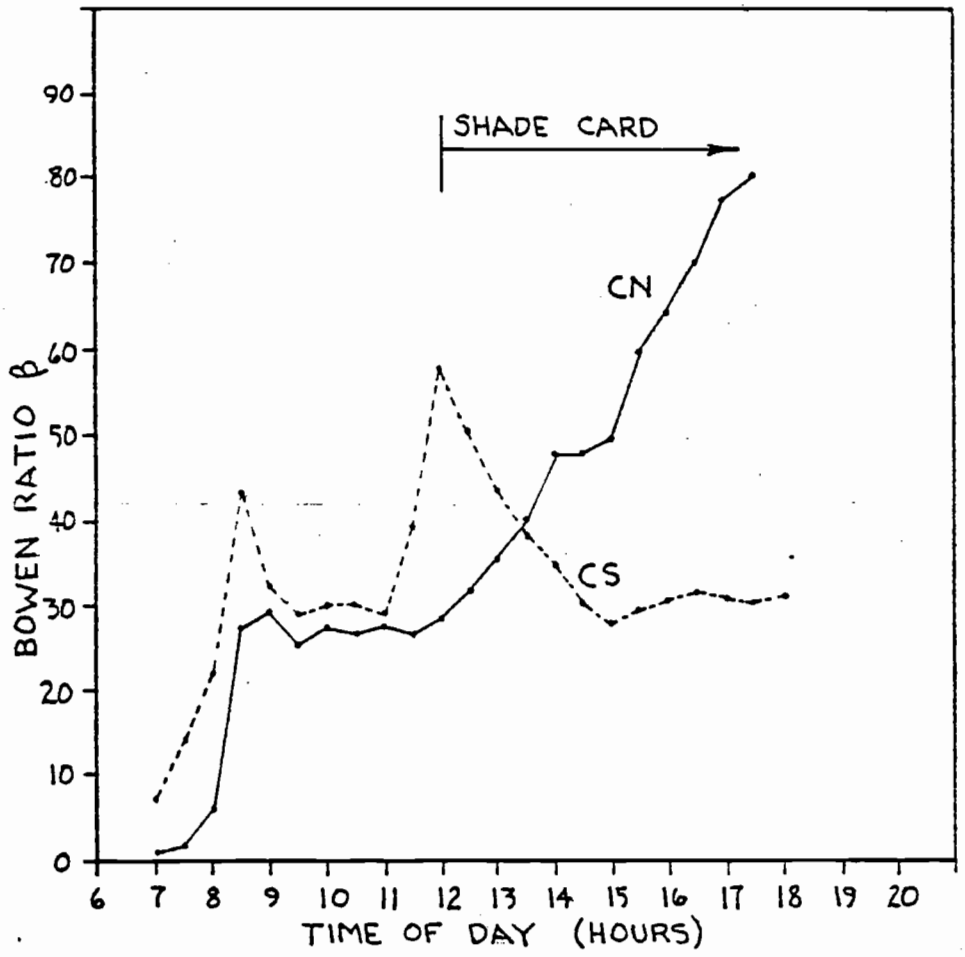

Figure 5. Daily pattern in the Bowen ratio for seedlings CN and CS on August 7, 1981. The shadecard beside CS became effective at 1200.

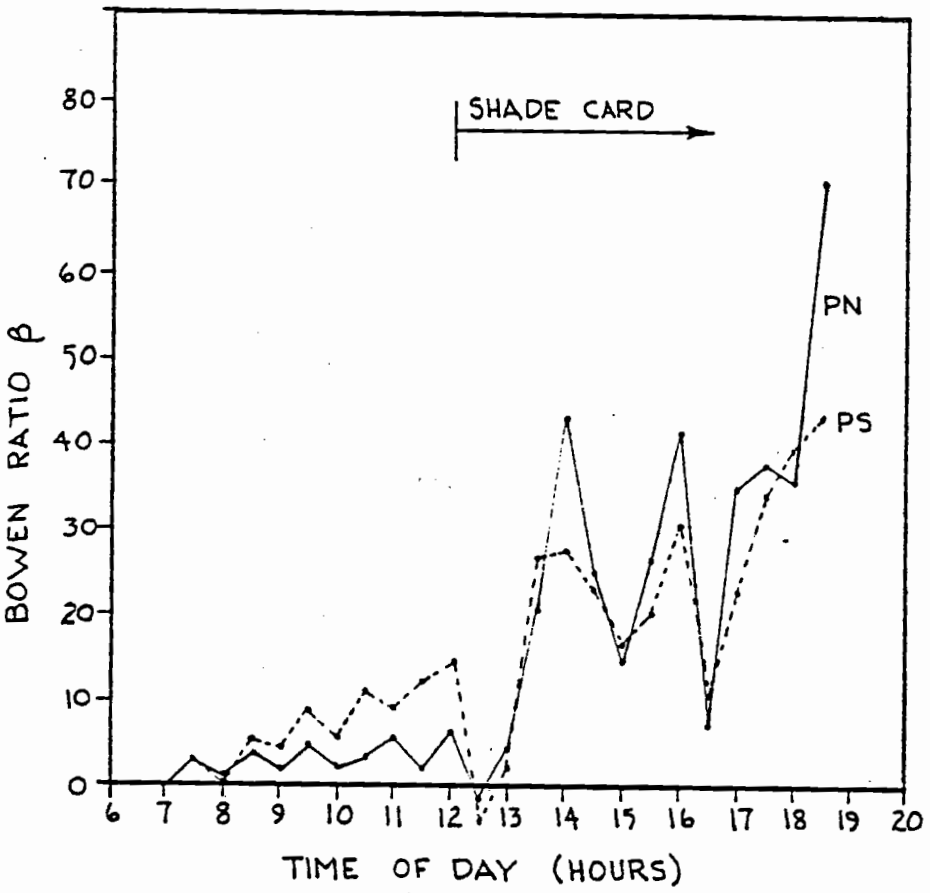

Figure 6. Daily pattern in the Bowen ratio for seedlings PN and PS on August 7, 1981. The shadecard beside PS became effective at 1200.

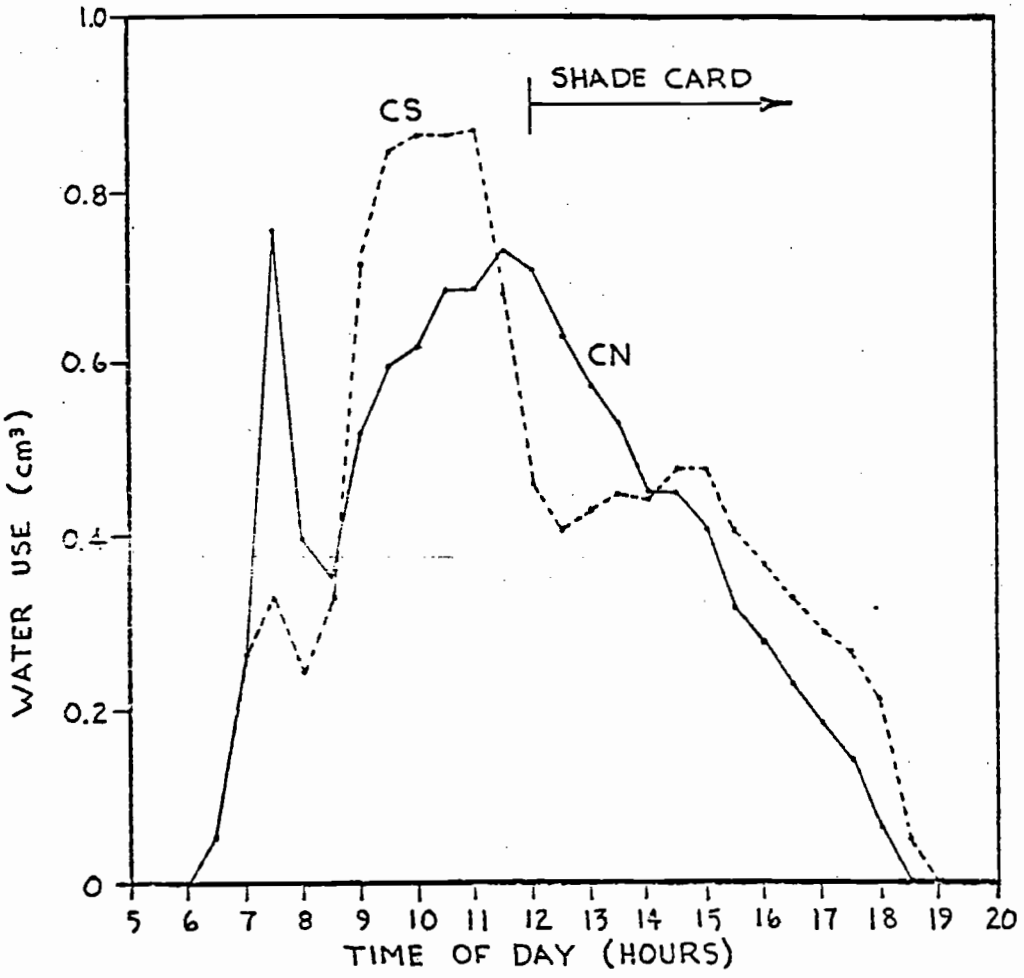

Figure 7. Daily pattern in water use for seedlings CN and CS on August 7, 1981. The shadecard beside CS became effective at 1200.

transplanted seedlings and, therefore, increasing the chance of survival during periods of heat and moisture stress.

For August 7, 1981, the partial-cut was found to have reduced the daily solar radiation incident to a seedling by 29%. This compares to a reduction of 22% by a shadecard alone, and 47% by a partial-cut/shadecard combination. The partial-cut was, therefore, slightly more effective, in a quantitative sense, than a shadecard in reducing the amount of solar radiation incident to a seedling.

The Bowen ratio increased greatly throughout the summer for the two seedlings on the clearcut, but very little for the two seedlings on the partial-cut. By late August, the seedlings in the clearcut had a sensible-to-latent heat loss ratio of between 40- and 60-to-1 while the seedlings in the partial-cut had ratios of only 10- and 15-to-1. There was a greater difference in the clearcut/partial-cut comparison than in either of the shadecard/no card comparisons. This indicates that the residual canopy of the partial-cut had a large effect upon the Bowen ratio, while the shadecard had little effect upon the Bowen ratio on either site.

The water use by the seedlings on the clearcut changed markedly over the summer with the greatest use in May and the least use in August. In contrast, the two seedlings in the partial-cut had the lowest use in May, with greater use in either July or early August. The early August period coincided with one of the worst "heat waves" on record and this may have helped magnify the differences between treatments. As with the Bowen ratio, there was a greater difference between water uses in the clearcut/partial-cut comparison than in either of the shadecard/no card comparisons.

There was a significant difference in total water use between the two sites. The seedlings on the clearcut used about half the amount of water that the seedlings on the partial-cut used. There was also a great difference in distribution of water use. For example, the seedlings on the clearcut used between 47 and 54% of their total summer water use in the May to July period compared to only 31 to 39% for the seedlings in the partial-cut. In contrast, the clearcut seedlings used only 10 to 12% of total water use in late August when the partial-cut seedlings used 18 to 23%. This suggests that the seedlings in the clearcut were not as active in water use as those in the partial-cut in the late summer. This may be a result of the clearcut seedlings being water stressed from a lack of available water.

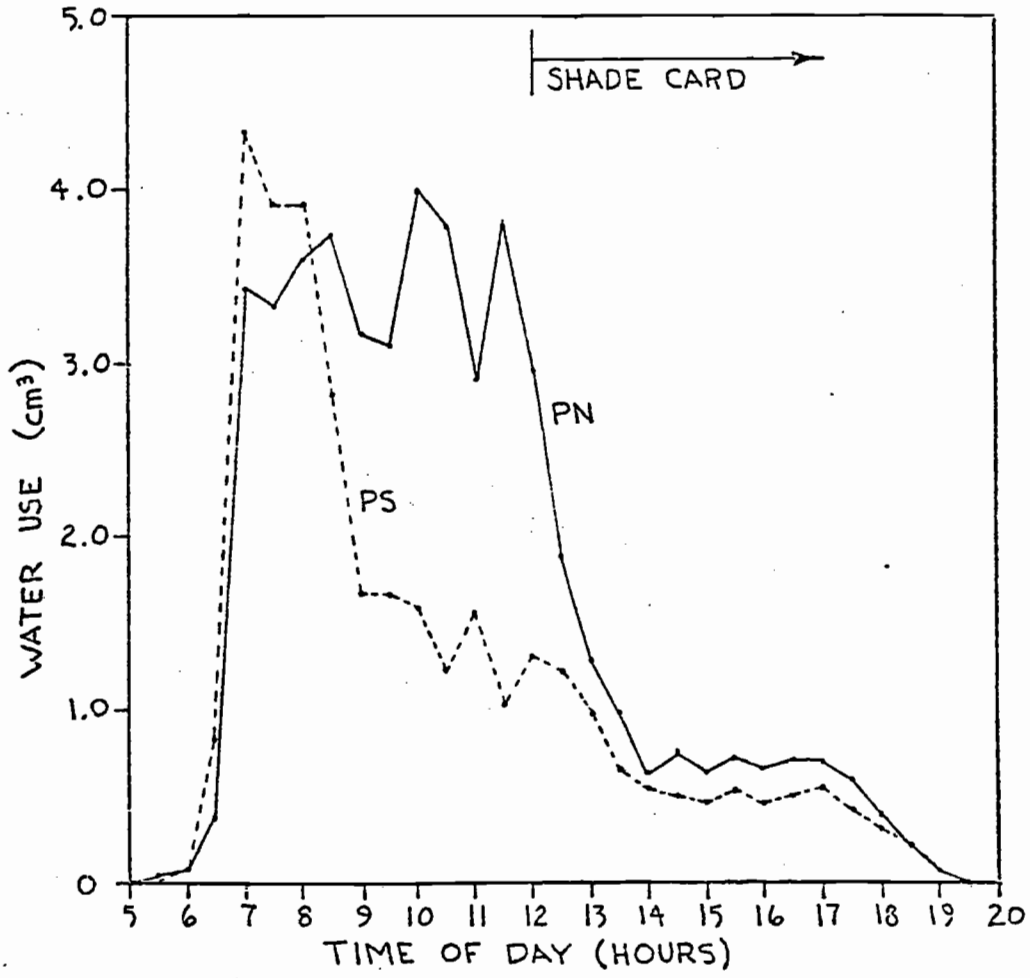

Figure 8. Daily pattern in water use for seedlings PN and PS on August 7, 1981. The shadecard beside PS became effective at 1200.

(~ 1.0 g/cm^3). The large decrease in water for CS (Figure 7) occurred between 1100 and 1200, before the shade card became effective, and remained somewhat constant throughout the afternoon.

A similar pattern is revealed in the water use for PS (Figure 8) except that its decrease occurs much earlier, between 0800 and 0900. It also remains somewhat constant in the afternoon. LE (water use) holding steady through 1200 and into the afternoon for CS and PS implies that the large decrease in β for both of these seedlings at 1200 is a result of a change in H, the sensible heat loss.

This constancy in LE relative to H might be explained by the different time responses of the needle to changes in moisture and thermal inputs. Stomata respond to a change in the internal water status of the needle via several different feedback mechanisms. This stomatal response is on the order of several minutes (Raschke, 1975). Needle temperature, however, responds even faster, on the order of seconds to a couple of minutes (Monteith, 1981). Thus, there appears to be a greater tendency for H, a function of the needle-airspace temperature difference, to change in response to a change in Q* than for LE, a function of stomatal resistance, to change. On a daily basis the change in Q* tends to be balanced by changes in H. This does not appear to be the case over the summer as will be discussed next.

Summer Pattern of Water Use

The water use per unit leaf area during the summer of 1981 is shown in Figure 9 for all four seedlings. It is evident that water use and, therefore LE, decreased over the summer for the

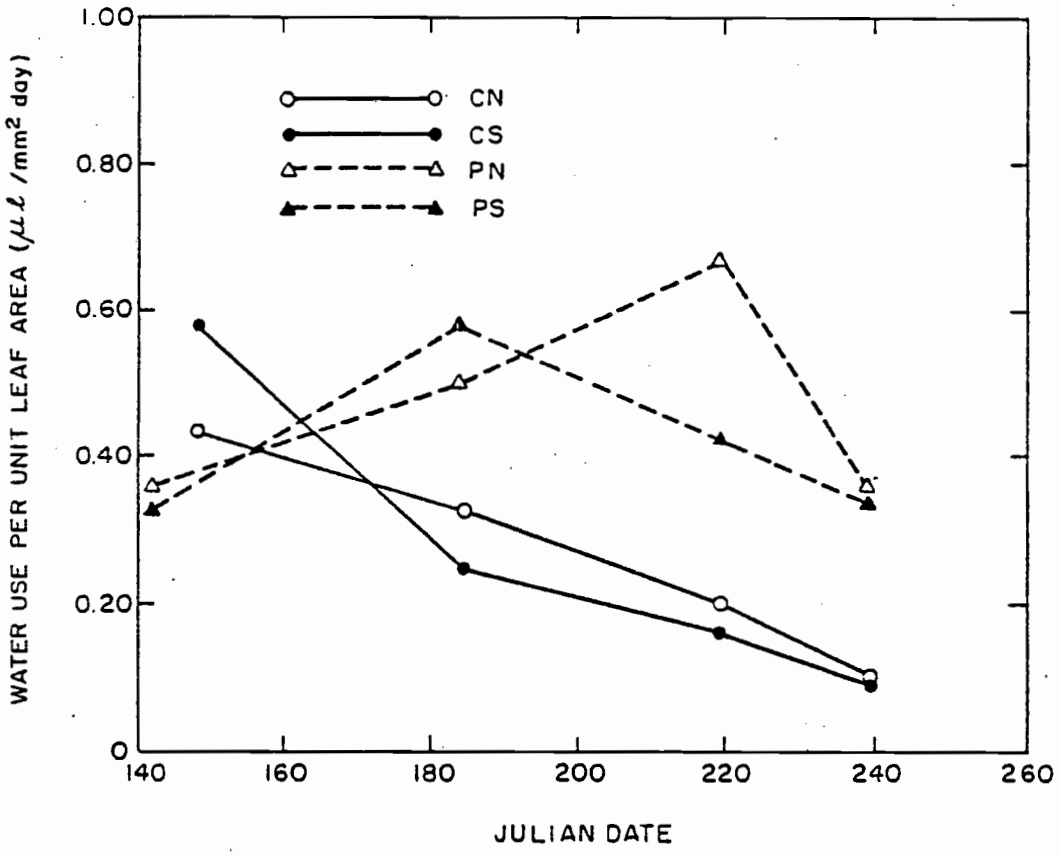

Figure 9. Seasonal trend in water use of four Douglas-fir seedlings on two cut-over sites in southwest Oregon in the summer of 1981. (C = clearcut, P = partial-cut, N = no card, and S = shadecard.)

seedlings in the clearcut, but not for seedlings in the partial-cut. Table 3 also reveals that H changed proportionately less than LE over the summer period. On a seasonal basis the change in Q* tends to be balanced more by a change in LE than in H. This is different from that described above for the diurnal patterns. The change in LE probably reflects a decreasing amount of water available for use by the seedlings on the clearcut. This is not the case in the partial-cut, as LE remained somewhat constant throughout the summer.

Figure 9 also shows that the difference in water use (and LE) between sites is generally greater than the difference between seedlings on a site. This shows that the difference between the clearcut and partial-cut treatments is greater than the difference between the shade card/no card comparisons.

The total water use by each seedling for the summer was also calculated and is shown in Figure 10 as average water use per day (cm^3/day) and in Figure 11 as the total amount used over the summer (cm^3). It must be emphasized, however, that this is the maximum amount of water that could be expected to be used. Since the four days chosen for calculations had mostly cloudless conditions, the amount of water actually used is expected to have been less than that calculated and shown in Figure 11.

Figures 10 and 11 show that there was little difference in total water use between seedlings on a site, but that there was a large difference between sites. As explained earlier, this is probably the upper limit, with the actual total somewhat less. Assuming that the seedling roots occupy a cylindrical volume, estimates of the amount of water that would be available can be made. If the dimensions of the

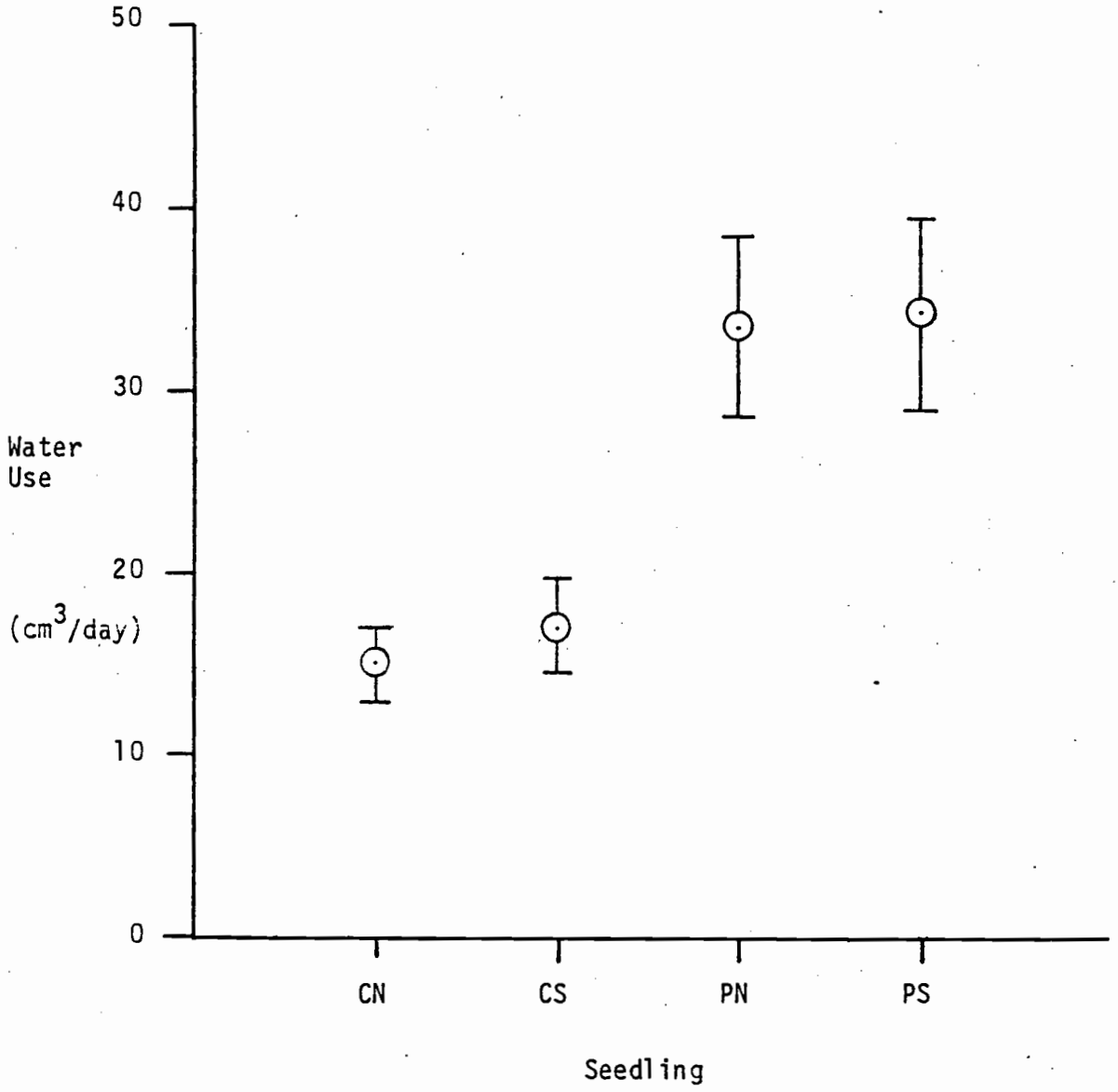

Figure 10. Mean daily water use of four seedlings for the summer of 1981. Vertical lines indicate the 15% error level in measurements of water use.

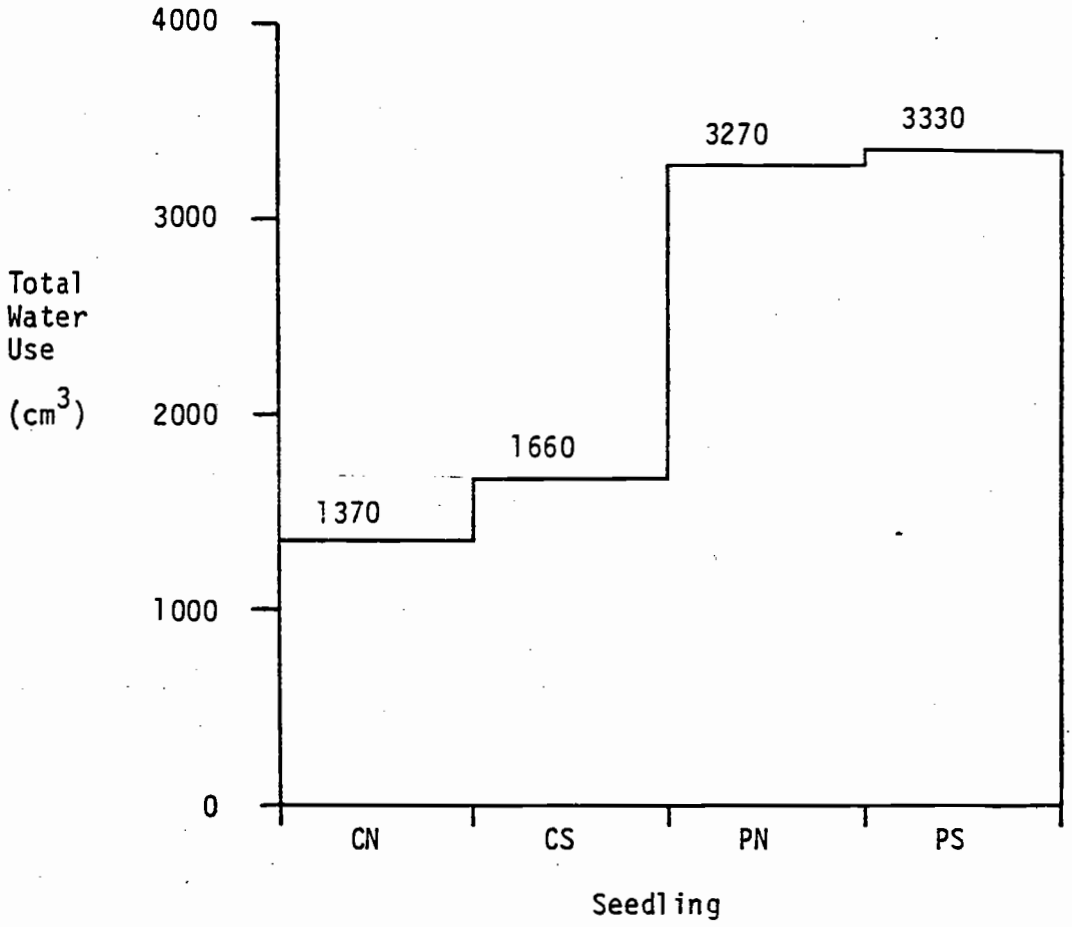

Figure 11. Total water use of four seedlings for the summer of 1981.

auger hole (radius = 10 cm, depth = 30 cm) are used, the total soil volume is $\pi r^2 d$, or 9400 cm^3 for the auger hole volume. Flint (198X) found the water-holding content of the soils on this site to be about 0.20 for water potentials between -0.01 MP_a (field capacity) and -3.0 MP_a (lower limit for Douglas-fir). Thus, the amount of water available in an auger hole volume of soil is 1880 cm^3, only enough to supply the total amounts shown in Figure 11 for the seedlings on the clearcut. It would not be enough for the partial-cut seedlings without either root extension or soil water transport to the seedling location. There is little evidence, however, that would suggest that Douglas-fir seedlings do not extend roots beyond the auger hole volume their initial year after outplanting. Indeed, when the seedlings were dug up at the end of the field season (late August), it was noted that several roots were found beyond the limits of the original auger hole. Root extension has been shown to be an effective drought avoidance strategy from both theoretical considerations (Caldwell, 1976) and field studies of saltbush [Atriplex confertifolia (Torr. & Frem.) Wats.] (Fernandez and Caldwell, 1975) and cotton (Gossypium hirsitum) (Hillel, 1971; Klepper et al., 1973; Taylor and Klepper, 1974). Studies in conifers (Leaphart and Wicker, 1966; Kaufmann, 1968; Kaufmann, 1977; Leshem, 1965) have also given evidence that root extension does occur during the summer drying period, although at greatly reduced rates. The experience of field foresters also needs to be considered. Examinations of many outplanted Douglas-fir seedlings have shown that roots do extend beyond the auger hole, especially if the soil is low in clay and if favorable spring weather follows planting (Karen Jones, personal communication. Both of these

conditions were realized on the Cave Creek site in 1981. It is expected, therefore, that the seedlings did occupy a soil volume larger than the auger hole, so that the water use numbers in Figure 11 are not gross overestimates. Even a small increase in the radius of the cylinder, from 10 to 12 cm, will cause a large increase in available water. A cylinder of r = 12 cm and d = 30 cm will have 2700 cm^3 of water, an increase of 44% over the cylinder of 10-cm radius.

The fractional distribution of the total water use was calculated for each of the three summer periods (Table 5). These periods were defined as Julian Dates 148-185, 185-219, and 219-239 for the clearcut and Julian Dates 142-184, 184-219, and 219-239 for the partial-cut. The summer period, thus, was a total of 91 days for the clearcut and 97 days for the partial-cut. This fractional distribution (Table 5) shows that around 50% of the summer water use by the seedlings in the clearcut occurred in the May to July period (JD 148-185). In contrast, the seedlings in the partial-cut had a more uniform water use distribution. The clearcut seedlings used less than 12% of the water after the heat wave of early August, whereas the partial-cut seedlings used 23% and 18%, respectively, of the water in this same period.

Water Use During Heat Wave

Differences in water use between the sites were magnified during the August, 1981 heat wave. This week-long period was characterized at the site by air temperatures exceeding 37°C (100°F) every day with maximum seedling airspace temperatures over 40°C (104°F) (unpublished

Table 5. Fractional distribution of water use occurring within each of three summer periods.

Seedling	% of Total		
	May to July use	July to August use	Late August use
CN	47	41	12
CS	54	36	10
PN	31	46	23
PS	39	43	18

data). There was also an increase in the mean daily soil temperatures which would increase the amount of longwave radiation flux to the seedlings.

The diurnal pattern of water use during the heat wave (August 7), shown earlier in Figures 7 and 8 for both sites, shows the greater amount of water use by the partial-cut seedlings over the clearcut seedlings as evidenced by the differences in scale along the ordinate (water use in cm^3). A small amount of this difference can be explained as a slight difference in the total leaf area since water use is not plotted per unit area, but the main reason is in the amount of water use. Much of this can be explained by the stomatal resistances measured on the sites. Figures 12 and 13 show the stomatal resistance patterns for the clearcut (Figure 12) and partial-cut (Figure 13) on August 7, 1981. These figures show that the stomatal resistances were lower on the partial-cut, especially after 1400, when those on the clearcut increased sharply while those on the partial-cut decreased. Stomata are usually thought to respond to changes in internal water status (Raschke, 1975; Running, 1976) which is affected by the availability of soil water (Tan and Black, 1976). There has been some evidence, however, that stomata can respond directly to vapor density deficits between the leaf and the air, especially for current-year needles (Cowan, 1977; Meinzer, 1982a). If this is the case, the vapor density deficit could have somewhat of a balancing effect, increasing the driving force behind transpiration on one hand (see Equation 4) and increasing the resistance to water flow on the other hand, by causing an increase in stomatal resistance. The lower stomatal resistances in the partial-cut may, therefore, reflect the

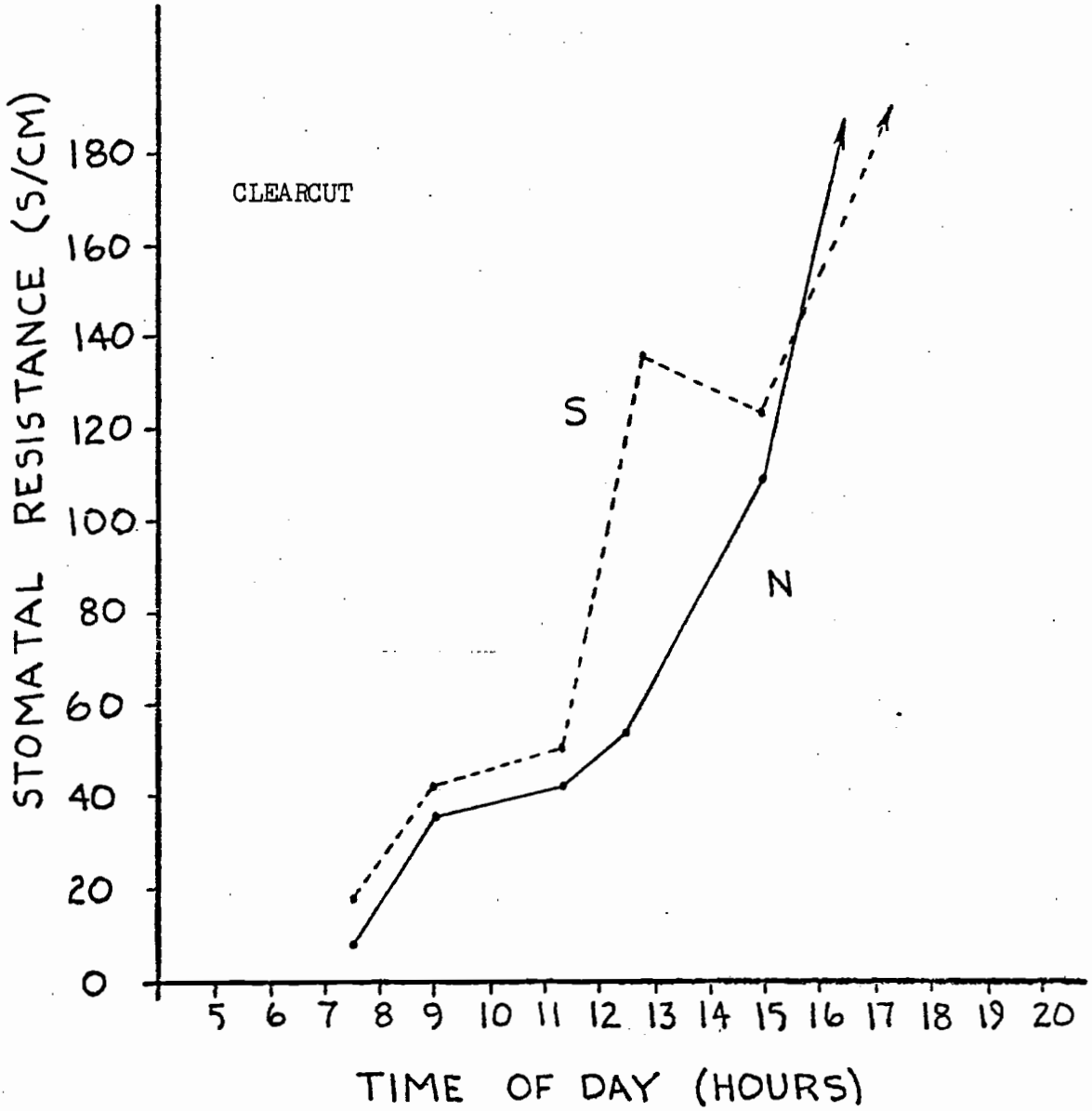

Figure 12. Stomatal resistance patterns of seedlings on the clearcut with shadecards (S) and without shadecards (N) on August 7, 1981.

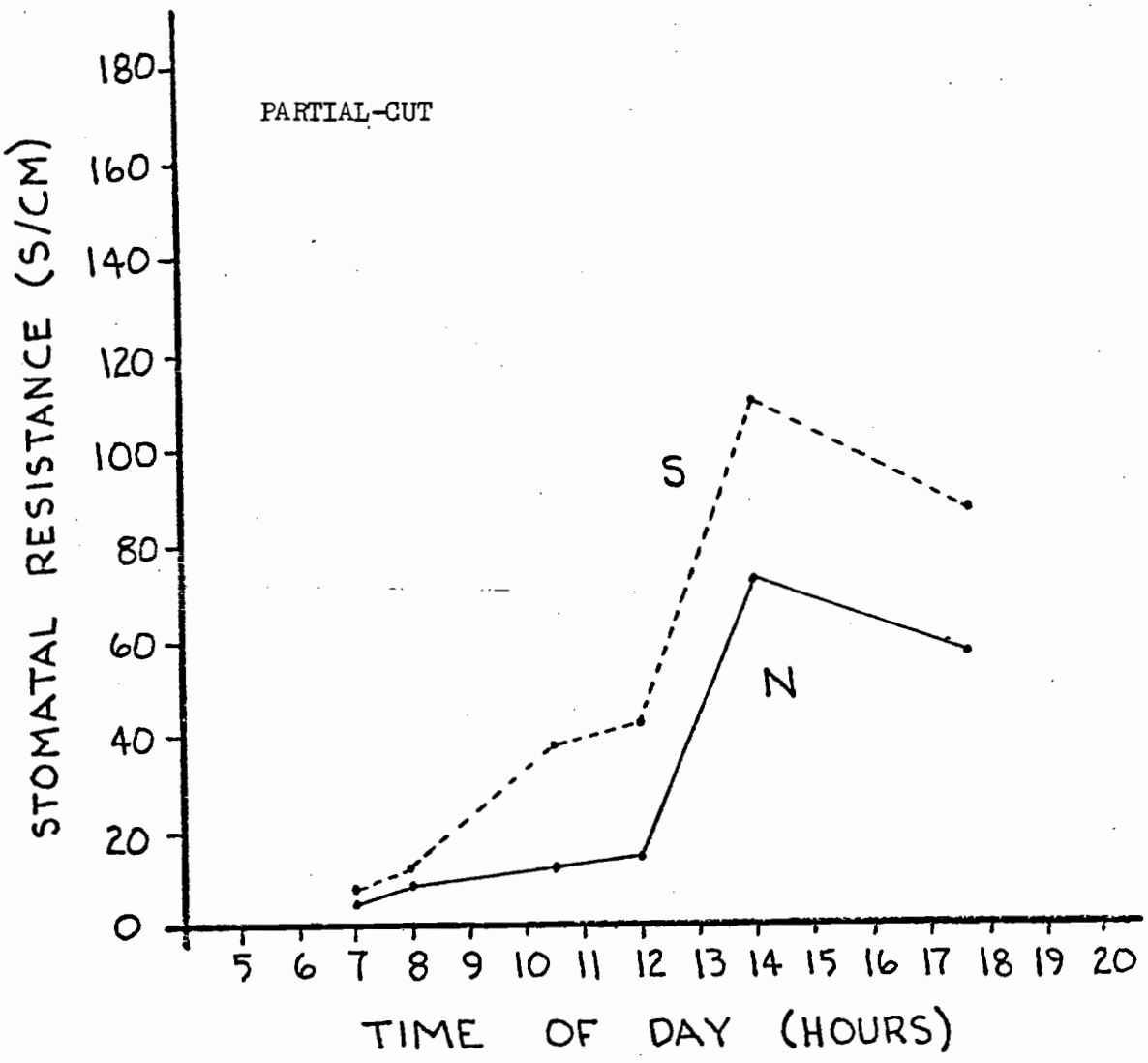

Figure 13. Stomatal resistance patterns of seedlings on the partial-cut with shadecards (S) and without shadecards (N) on August 7, 1981.

presence of either lower vapor density differences, more available soil water, or a combination of both. It is believed to be the combination although no daily measurements of soil water are available which would allow validation.

A surprising feature of Figures 12 and 13 is that the stomatal resistances were lower for the seedlings without shade cards than those with cards. Since each point on the figures represent the mean of three different seedlings, the feature is probably typical. Meinzer (1982b) has shown Douglas-fir stomata to increase in resistance with decreasing light levels. Whether the decrease in light behind a shade card is enough to cause an increase in stomatal resistance is unknown. This seems doubtful, however, because the patterns in Figures 12 and 13 remain constant throughout the day with no obvious changes around 1200 (when the shade cards become effective) which would suggest a light level control of stomatal resistance.

Applications to Reforestation

Any time reforestation is delayed following harvesting, a loss is incurred in both economic value and volume yield (Brodie and Tedder, 1982). This fact often justifies the costs of techniques used to speed reforestation. Since heat and moisture stress have been implicated as major reasons for reforestation failure on cutover sites (Strothmann, 1976; Minore 1978; Hobbs et al., 1979; Helgerson et al., 1982) any reforestation technique which can improve seedling survival by either reducing the heat loading on, or improving the water use by, seedlings is desirable.

The results from this study show that the partial-cut was more effective than the shadecards in providing shade, in changing the partitioning of net radiation, and in improving the distribution of water use over the summer for four transplanted Douglas-fir seedlings. The two seedlings on the partial-cut also used significantly more water over the summer than those on the clearcut. The residual canopy of the partial-cut reduced the solar radiation incident to a seedling slightly more (27% vs. 22%) than a shadecard. What may be more important, though is the amount of soil-plant-air volume which is affected by that shade. The shade from a residual canopy covers a larger volume which effects a lowering of the site air temperature and lowers the atmospheric demand for water as reflected by the vapor density deficit. Recent studies have shown that stomatal resistance can be affected directly by vapor density deficit (Cowan, 1977; Meinzer, 1982a). The lower stomatal resistances found in the partial-cut may be a result of the lower vapor density deficits found in the

partial-cut (unpublished data). This way, the type of elements making up the shade (i.e., large vs. small elements) could have an indirect effect upon stomatal resistance and, therefore, water use and CO_2 uptake. The large difference in total water use between the two sites probably results from these differences in stomatal resistance.

The residual canopy also appeared to effect a change in the partitioning of net radiation (Q*). The β values for the two partial-cut seedlings increased only slightly over the summer indicating a constancy between H and LE. In contrast, β increased greatly over the summer for the clearcut seedlings. This large change in the clearcut possibly indicates increasing water stress since H became so large relative to LE.

The results also show that the seedlings in the partial-cut had a much better pattern of water use with regard to survival. Water use was more evenly spread throughout the summer than for the clearcut seedlings, and the highest use occurred in mid- to late-summer when moisture stress would be more likely to occur. If the water use pattern of the partial-cut could be induced in clearcuts without using the shelterwood method, perhaps that distribution would result in better survival and lower stresses.

Shade has been shown to increase seedling survival. Shadecards have improved survival on soils with low water-holding capacity (Lewis et al., 1978), under drought conditions (Woodard, 1966; Baer et al., 1977), and on soils with high coarse fragment content (Hobbs, 1982; Petersen, 1982). This was also the case in this study. A survival survey in October, 1981 (unpublished data), showed 56% survival (34 of 61) on the clearcut compared to 98% (60 of 61) on the partial-cut. On

the clearcut, 72% (23 of 32) of the seedlings with shadecards survived while only 38% (11 of 29) of those seedlings without shadecards survived. Another survey in May, 1982, found that only 17% of the seedlings on the clearcut without cards survived the first year, while the remaining survival percentages remained about the same. While shade cannot add soil moisture to a droughty site, it can possibly cause a decrease in the transpirative demand, and therefore, effect a conservation in the use of water that is available. Woodard (1966) showed that shade from shadeframes prolonged the survival period of Douglas-fir seedlings which lacked available soil moisture. In the case of heat waves, a few days can make the difference. A survival survey in the clearcut on August 26, two weeks after the heat wave, showed that of the 18 unshaded seedlings dead in October, 9 had died by August 26. In contrast, of the 9 shaded seedlings dead in October, none had died by August 26. Thus, for this study, there appears to be a shadecard-induced postponement of seedling death.

High soil temperatures are believed to have killed many of the seedlings in the clearcut (Miller et al., 1982). That is probably one reason why no major differences occurred in the energy balance terms (either β or water use) between CN and CS even though there was such a large difference in survival between unshaded and shaded seedlings on the clearcut. Also, had an energy balance analysis been done on one of the dead or dying seedlings, there probably would have been a large difference.

The results from this study must be tempered by the fact that the heat wave of early August was an event with a somewhat low probability of occurrence. This could be looked upon as of both positive and

negative consequence. Since a heat wave is of low occurrence, there may be a tendency to overexaggerate the poor results of certain treatments. On the other hand, there are usually very few opportunities to make field measurements under such severe conditions and, therefore, the extremes in regard to seedling microclimate are unknown. The difference between sites was enhanced as a result of the heat wave, and also allowed a delineation of energy balance terms under extreme conditions of water and heat stress.

CONCLUSIONS

1. Incoming solar radiation to transplanted Douglas-fir seedlings was reduced by 22% with a shade card, by 29% with a residual canopy, and by 47% with a combination of the two.
2. The solar radiation received by a Douglas-fir seedling was calculated by a model simulating seedling geometry, by a spherical PAR sensor, and by a horizontally-oriented pyranometer. The model and PAR compared favorably and the agreement is probably sufficient to allow either the representation of a seedling as a sphere, or the use of a PAR sensor to measure incoming radiation to seedlings. The pyranometer, however, compared poorly with the model and shows the error in attempting to measure incoming solar radiation to three-dimensional objects with two-dimensional sensors.
3. Although the shade card and residual canopy are about equal with respect to the reduction in magnitude of incoming solar radiation, there is a difference in the timing and type of shade provided. The shade from a residual canopy covers a larger soil-plant-air volume which effects a lowering of the site air temperature more than the shade from a shadecard. This possibly lowers the atmospheric demand for water as reflected by the vapor density deficit which can directly affect stomatal resistance.
4. Net radiation received by Douglas-fir seedlings is partitioned mainly into convective, sensible heat loss rather than as latent heat loss (transpiration). This results in Bowen ratios that are very much higher than those measured over forest canopies.
5. The Bowen ratio increases greatly during the summer for seedlings growing in a clearcut but not for seedlings growing in a

partial-cut (shelterwood). The high β values for the clearcut in August indicate that the seedlings are probably under stress, since the heat loss by convection is up to 60 times that lost by transpiration. The subsequent death of seedlings on the site also substantiates this. Water was probably limiting on the site this time.

6. The difference in the Bowen ratio is greater between sites (partial-cut/clearcut) than between the shade card/no card comparisons. This quantifies the effect that a partial-cut makes a greater improvement in seedling welfare than does a shade card.
7. Water use by seedlings in the clearcut decreased between May and July and was low the remainder of the summer. In contrast, water use by seedlings in the partial-cut increased between May and July or early August. The highest measured use in the clearcut was in May while the highest measured use in the partial-cut occurred in July and early August.
8. The two seedlings in the partial-cut used about twice as much water as the clearcut seedlings during the summer of 1981. This resulted from lower stomatal resistances in the partial-cut which arose from lower vapor density deficits and, possibly, higher soil moisture levels.
9. The differences in water use, as with β, was greater between the partial-cut/clearcut comparison than between either of the shade card/no card comparisons. This also suggests that the partial-cut makes more of an improvement in the distribution of water use than the shade card. The even distribution of water use in the partial-cut (31-39% early, 43-46% mid, and 18-23% late) would tend

to favor the survival of seedlings by the availability of water in the later part of the summer drought period. The uneven distribution of water use on the clearcut (47-54% early, 36-41% mid, and only 10-12% late) shows a rapid use of water early with the possible lack of availability late in the summer drought period which could lead to moisture stress.

REFERENCES CITED

Baer, N., F. Ronco, and C. W. Barney. 1977. Effects of watering, shading, and size of stock on survival of planted lodgepole pine. U.S.D.A. Forest Service, Rocky Mtn. For. and Range Exp. Sta., Research Note RM-347. 4 pp.

Beardsell, M. F., P. G. Jarvis, and B. Davidson. 1972. A null-balance diffusion porometer suitable for use with leaves of many shapes. J. Appl. Ecol. 9:677-690.

Brodie, J. D., and P. L. Tedder. 1982. Regeneration delay: economic cost and harvest loss. J. For. 80:26-28.

Caldwell, M. M. 1976. Root extension and water absorption. In: Ecological Studies. analysis and Synthesis, Vol. 19: Water and Plant Life, (ed.) O. L. Lange, L. Kappen, and E. D. Schulze. Springer-Verlag, Berlin. pp. 63-85.

Campbell, G. S. 1977. An Introduction to Environmental Biophysics. Springer-Verlag, New York. 159 pp.

Childs, S. W., H. R. Holbo, and E. L. Miller. 198X. Shadecard and shelterwood modification of the soil temperature environment. Submitted to Forest Science.

Cowan, I. R. 1977. Stomatal behavior and environment. Adv. Bot. Res. 4:117-227.

Fernandez, O. A., and M. M. Caldwell. 1975. Phenology and dynamics of root growth of three cool semi-desert shrubs under field conditions. J. Ecology 63:703-714.

Flint, A. F. 198X. Physical properties of coarse fragments and their effect on available water in skeletal soils. Manuscript submitted to Soil Sci. Soc. Am. J.

Fritschen, L. J., R. B. Walker, and J. Hsia. 1980. Energy balance of an isolated Scots pine. Int. J. Biometeorol. 24:293-300.

Gates, D. M. 1963. Leaf temperature and energy exchange. Arch. Met. Geophys. u. Bioklim. (Berlin) 12:321-336.

Gay, L. W., and H. R. Holbo. 1971. Evapotranspiration study - Malheur Lake, Silvies River Drainage. Oregon State University, Corvallis, Oregon. Final Report, Corps of Engineers, Contract No. DACW 68-72-C-0032. 21 pp.

Gay, L. W., and J. B. Stewart. 1974. Energy balance studies in coniferous forests. Report No. 23, Instit. Hydrol., Natural Environ. Res. Council, Wallingford, Berks.

Halverson, H. G., and D. F. Potts. 1981. Water requirements of honeylocust (Gleditsia triacanthos f. inermis) in the urban forest. U.S. Dept. Agric., Forest Service, Research Paper NE-487. 4 pp.

Helgerson, O. T., K. A. Wearstler, Jr., and W. K. Bruckner. 1982. Survival of natural and planted seedlings under a shelterwood in southwest Oregon. Oregon State University, Forest Res. Lab., Res. Note 69. 4 pp.

Hillel, D. 1971. Soil and Water: Physical Principles and Processes. Academic Press, New York. 288 pp.

Hobbs, S. D., D. M. McNabb, and K. A. Wearstler, Jr. 1979. Annual report to cooperators (October 1, 1978-September 30, 1979). Southwest Oregon Forestry Intensified Research Program. Oregon State University, For. Res. Lab. 111 pp.

Hobbs, S. D., R. H. Byars, D. C. Henneman, and C. R. Frost. 1980. First-year performance of 1-0 containerized Douglas-fir seedlings on droughty sites in southwestern Oregon. Oregon State University, For. Res. lab. Res. Paper 42. 15 pp.

Hobbs, S. D. 1982. Performance of artificially shaded container-grown Douglas-fir seedlings on skeletal soils. Oregon State University, For. Res. Lab., Research Note 71. 6 pp.

Holbo, H. R. 1973. Energy exchange studies at the earth's surface. II. Energy budget of a pumice desert. Dept. Atmos. Sci. Tech. Note No. 73-II, Oregon St. Univ., Corvallis, Oregon. 142 pp.

Holbo, H. R. 1981. A dew-point hygrometer for field use. Agric. Meteorol. 24:117-130.

Holbo, H. R., S. W. Childs, and E. L. Miller. 198X. Summertime radiation balances of logged and partly-logged slopes in southwest Oregon. Submitted to Forest Science.

Jarvis, P. G., G. B. James, and J. J. Landsberg. 1976. Chpt. 7. Coniferous forest. In: Vegetation and the Atmosphere, Vol. 2 (ed.) J. L. Monteith, Academic Press, London. pp. 171-240.

Kaufmann, M. R. 1968. Water relations of pine seedlings in relation to root and shoot growth. Plant Physiol. 43:281-288.

Kaufmann, M. R. 1977. Soil temperature and drought effects on growth of Monterey pine. For. Sci. 23:317-325.

Klepper, B., H. M. Taylor, M. G. Huck, and E. L. Fiscus. 1973. Water relations and growth of cotton in drying soil. Agron. J. 65: 307-310.

Knoerr, K. R. 1967. Contrasts in energy balances between individual leaves and vegetated surfaces. In: International Symposium on Forest Hydrology, (eds.) W. E. Sopper and H. W. Lull, Pergamon Press, London. pp. 391-401.

Knoerr, K. R., and L. W. Gay. 1965. Tree leaf energy balance. Ecol. 46:17-24.

Leaphart, C. D., and E. F. Wicker. 1966. Explanation of pole blight from responses of seedlings grown in modified environments. Can. J. Bot. 44:121-137.

Leshem, B. 1965. The annual activity of intermediary roots of the Aleppo pine. For. Sci. 11:291-298.

Lewis, R., C. J. Ritter, Jr., and S. Wert. 1978. Use of artificial shade to increase survival of Douglas-fir in the Roseburg area. U.S. Dept. Int., Bur. Land Mgmt., Tech. Note 321. 8 pp.

Mann, J. E., G. L. Curry, and P. J. H. Sharpe. 1979. Light interception by isolated plants. Agric. Meteorol. 20:205-214.

McNaughton, K., and T. A. Black. 1973. A study of evapotranspiration from a Douglas-fir forest using the energy balance approach. Water Resources Research 9:1579-1590.

Meinzer, F. C. 1982a. The effect of vapor pressure on stomatal control of gas exchange in Douglas-fir (Pseudotsuga menziesii) saplings. Oecologia (Berlin) 54:236-242.

Meinzer, F. C. 1982b. The effect of light on stomatal control of gas exchange in Douglas-fir (Pseudotsuga menziesii) saplings. Oecologia (Berlin) 54:270-274.

Miller, P. C. 1967. Leaf temperatures, leaf orientation and energy exchange in quaking aspen (Populus tremuloides) and Gambell's oak (Quercus gambellii) in central Colorado. OEcol. Plant. 2:241-270.

Miller, E. L., S. W. Childs, and H. R. Holbo. 1982. Heat wave, 1981. Soil temperatures and seedling mortality. Oregon State Univ. Extension Service, FIR Report 4(1):5-6.

Minore, D. 1971. Shade benefits Douglas-fir in southwestern Oregon cutover area. Tree Plant. Notes 22(1):22-23.

Minore, D. 1978. The Dead Indian Plateau: A historical summary of forestry operations and research in a severe southwestern Oregon environment. U.S.D.A. Pacific NW For. and Range Exp. Sta. Gen. Tech. Rep. PNW-72. 23 pp.

Monteith, J. L. 1973. Principles of Environmental Physics. Edward Arnold, London, England. 241 pp.

Monteith, J. L. 1981. Coupling of plants to the atmosphere. In: Plants and Their Atmospheric Environment, (eds.) J. Grace, E. D. Ford, and P. G. Jarvis. Blackwell Scientific Publ.

Moore, C. J. 1976. Eddy flux measurements above a pine forest. Quart. J. Royal Met. Soc. 102:913-918.

Murphy, C. E., Jr., J. F. Schubert, and A. H. Dexter. 1981. The energy and mass exchange characteristics of a loblolly pine plantation. J. Appl. Ecol. 18:271-281.

Nobel, P. S. 1974. Boundary layers of air adjacent to cylinders. Plant Physiol. 54:177-181.

Norman, J. M., and P. G. Jarvis. 1974. Photosynthesis in Sitka spruce [Picea sitchensis (Bong.) Carr.]. III. Measurements of canopy structure and interception of radiation. J. Appl. Ecol. 11:375-398.

Oke, T. R. 1978. Boundary Layer Climates. Methuen & Co., London, England. 372 pp.

Oke, T. R. 1979. Advectively-assisted evapotranspiration from irrigated urban vegetation. Boundary-Layer Meteorol. 17:167-173.

Petersen, G. J. 1982. The effects of artificial shade on seedling survival on western Cascade harsh sites. Tree Planters' Notes 33(1):20-23.

Raschke, K. 1975. Stomatal action. Ann. Rev. Plant Physiol. 26:309-340.

Running, S. W. 1976. Environmental control of leaf water conductance in conifers. Can. J. For. Res. 6:104-112.

Ryker, R. A., and D. R. Potter. 1970. Shade increases first-year survival of Douglas-fir seedlings. U.S.D.A. Forest Service Int. For. and Range Exp. Sta. Res. Note INT-119.

Scarborough, J. B. 1966. Numerical Mathematical Analysis. The Johns Hopkins Press, Baltimore. 600 pp.

Seidel, K. W., and R. Cooley. 1974. Natural reproduction of grand fir and mountain hemlock after shelterwood cutting in central Oregon. U.S.D.A. Forest Service Pac. NW For. and Range Exp. Sta. Res. Note PNW-229. 10 pp.

Sinclair, T. R. 1972. Error analysis of latent, sensible and photochemical heat flux densities calculated from energy balance measurements above forests. In: Modeling the Growth of Trees, (eds.) C. E. Murphy, Jr., J. D. Hesketh, and B. R. Strain. EDFB-IBP 72-11, Oak Ridge Nat. Lab. pp. 55-66.

Sinclair, T. R., L. H. Allen, Jr., and E. R. Lemon. 1975. An analysis of errors in the calculation of energy flux densities above vegetation by a Bowen-ratio profile method. Boundary-Layer Meteorol. 8:129-139.

Strothmann, R. O. 1972. Douglas-fir in northern California: effects of shade on germination, survival, and growth. U.S.D.A. Forest Service Pac. SW For. and Range Exp. Sta. Res. Pap. PSW-84. 10 pp.

Strothmann, R. O. 1976. Douglas-fir seedlings planted by four methods...results after 10 years. U.S.D.A. Forest Service Pac. SW For. and Range Exp. Sta. Res. Note PSWE-310. 4 pp.

Tan, C. S., and T. A. Black. 1976. Factors affecting the canopy resistance of a Douglas-fir forest. Bound. Layer Meteor. 10:475-488.

Tanner, C. B., and E. R. Lemon. 1962. Radiant energy utilized in evapotranspiration. Agron. J. 54:207-212.

Taylor, H. M., and B. Klepper. 1974. Water relations of cotton. I. Root growth and water use as related to top growth and soil water content. Agron. J. 66:584-588.

Ungs, M. J. 1981. Distribution of light within the crown of an open-grown Douglas-fir. Unpublished Ph.D. Thesis, Oregon State University, Corvallis, Oregon.

Williamson, D. M., and D. Minore. 1978. Survival and growth of planted conifers on the Dead Indian Plateau east of Ashland, Oregon. U.S.D.A. Forest Service Pac. NW For. and Range Exp. Sta. Res. Pap. PNW-242. 15 pp.

Woodard, E. S. 1966. Effects of some transpiration retardants and shade on survival of Douglas-fir seedlings under drought conditions in the field. Unpublished M.S. Thesis, Oregon State University, Corvallis, Oregon. 30 pp.

APPENDIX A

Seedling Radiation Geometry

Douglas-fir seedlings can be modelled as an assemblage of needle-bearing cylinders. Conceptually, the mainstem is imagined as a vertically-oriented cylinder with cylindrical side branches extending outward from the mainstem (see Figure A1).

The incoming solar radiation geometry for the mainstem is shown in Figure A2. From this geometry, the projected area of the mainstem, A_{cyl}, along the sun-line is given by:

$$A_{cyl} = 2 \cdot r \cdot h \text{ SIN } Z_s + \pi r^2 \text{ COS } Z_s \qquad (A1)$$

where h is the length of the cylinder, r is the radius, and Z_s is the zenith angle of the sun. This area reduces to $2 \cdot r \cdot h$ when $Z_s = 90°$, and πr^2 when $Z_s = 0°$.

The radiation geometry for a side branch is shown in Figure A3. The angle α is determined by:

$$\text{COS } \alpha = \text{SIN } Z_s \text{ SIN } Z_b \text{ COS}(\theta_s - \theta_b) + \text{COS } Z_s \text{ COS } Z_b \qquad (A2)$$

where Z_b is the vertical angle of the branch, θ_b is the azimuth (horizontal angle) of the branch, θ_s is the azimuth of the sun, and α is the angle between the solar beam sunline and the main axis of the side branch. The angle α replaces Z_s in equation A1 to give the A_{cyl} for each side branch:

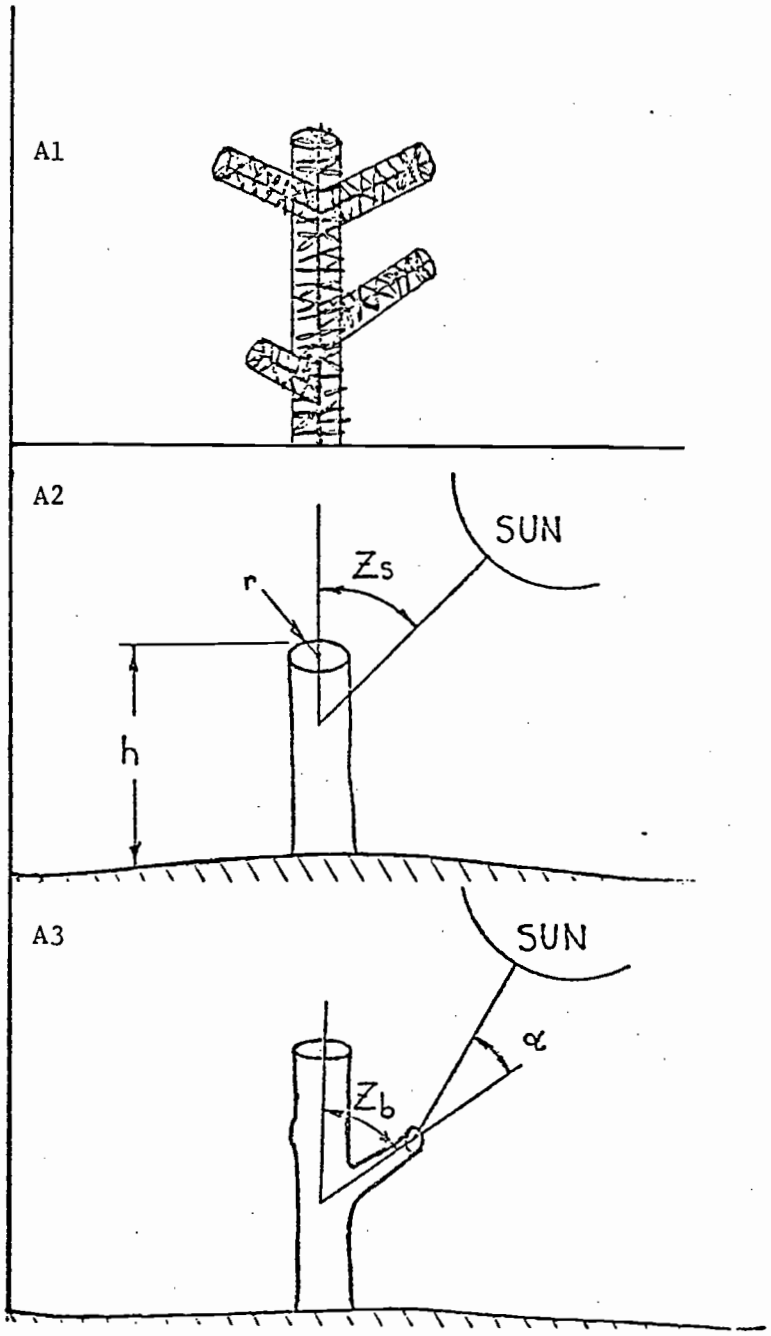

Figures A1-A3. Douglas-fir seedling radiation geometry. A1 - Seedling conceptualized as an assemblage of cylinders. A2 - Incoming solar radiation geometry for the mainstem. A3 - Incoming solar radiation geometry for a sidebranch.

$$A_{cyl} = 2 \cdot r \cdot h \text{ SIN } \alpha + \pi \, r^2 \text{ COS } \alpha \qquad \text{(A3)}$$

The total projected area of all branch-cylinders, therefore, requires measurements of the length, radius (needle length), and orientation of the mainstem and each branch. The solar position must also be determined to allow for the calculation of Z_s and θ_s throughout the day.

The solar position is determined by calculating the altitude and azimuth of the sun at any desired time. For this study, calculations were performed at half-hour intervals during the day. The solar altitude, A, of the sun above the horizon can be computed from:

$$\text{SIN } A = \text{SIN}\lambda \text{ SIN}\delta + \text{COS}\lambda \text{ COS}\delta \text{ COS } 15(t-t_o) \qquad \text{(A4)}$$

where λ is the latitude, δ is the solar declination on the day of calculations, t is the time of day in hours, and t_o is the time of the solar noon (Campbell, 1977).

The solar azimuth, θ_s, is computed from:

$$\theta_s = \text{COS}^{-1} \left(\frac{\text{SIN}\delta \text{ COS(LAT)} - \text{COS}\delta \text{ SIN(LAT) COS H}}{\text{COS A}} \right) \qquad \text{(A5)}$$

before solar noon, and by $360 - \theta_s$ after solar noon (Rao, 1981). H is the hour angle and is the same as term COS $15(t-t_o)$ in equation A4.

A subroutine, ALMANAC, was written which calculates the solar altitude and azimuth for half-hour increments throughout the day. Data requirements for the subroutine are the Julian Date (JD),

latitude (LAT) and longitude (LONG) of the site, and the time. The solar declination, δ, is computed from:

$$\delta = 0.40928 \text{ SIN}(4.88883 + 0.01721 \text{ JD}) \quad \text{(A6)}$$

The equation of time, ET, which corrects for the eccentricity and obliquity of the earth's orbit around the sun (Robinson, 1966), is determined from:

$$\text{ET} = \frac{0.7 \text{ SIN}(-0.986 \text{ JD}) + \text{SIN}(-1.97 \cdot \text{JD} - 15.78)}{6} \quad \text{(A7)}$$

The standard clock time is then corrected to "true" solar time by:

$$\text{SUNTIME} = \text{CLOCKTIME(PST)} + \text{ET} + \frac{(120.0 - \text{LONG})}{15} \quad \text{(A8)}$$

This solar time is the t used in equations A4 and A5 in calculating the hour angle for determining sun altitude and azimuth.

The only intraseedling shading considered was by that of the mainstem upon the side branches. The mainstem is the largest of all the cylinders and potentially provides the greatest amount of shade. Shading by the side branches is also possible, but would require a more complex mathematical description and computer model.

The shading of a side branch by the mainstem is accomplished by regarding a branch to be fully shaded when it is $180 \pm \phi°$ opposite in azimuth from the sun and below the shadow-line of the mainstem. This is described graphically in Figure A4. The angle ϕ is described by the horizontal geometry below in Figure A5. The angle is calculated by:

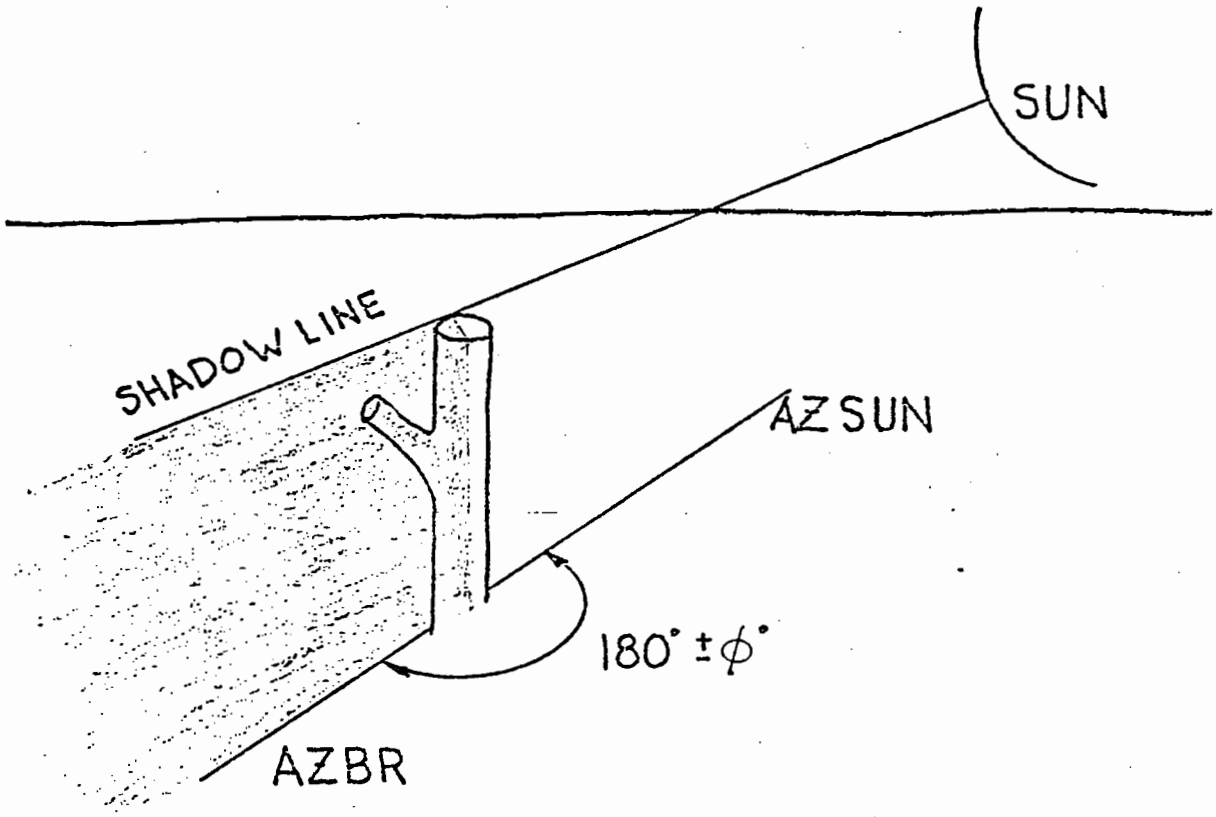

Figure A4. Geometrical determination of when a sidebranch is shaded by the mainstem.

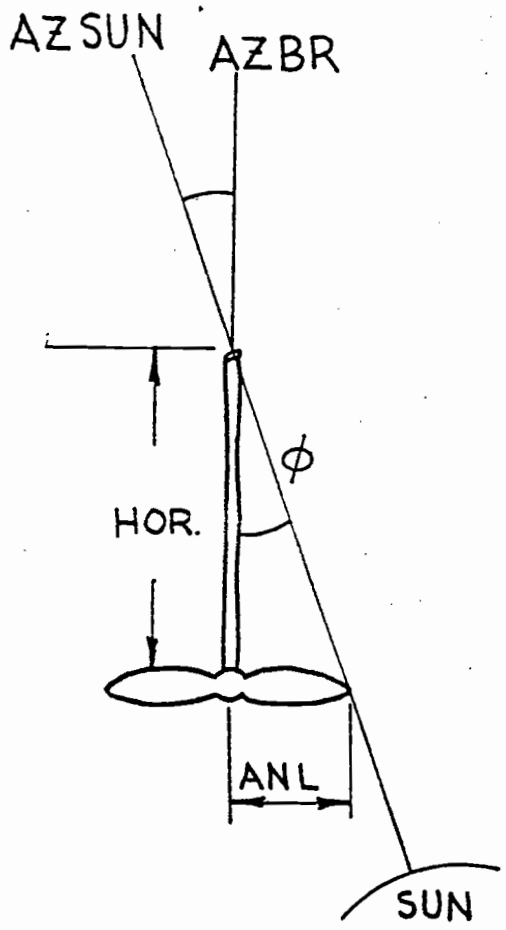

Figure A5. Horizontal shading geometry of a sidebranch.

$$\phi = \text{TAN}^{-1} \frac{\text{ANL}}{\text{HOR}} \tag{A9}$$

where ϕ is half the arc centered on 180° which comprises the shade envelope, ANL is the radius of the mainstem cylinder, estimated by the average needle length, and HOR is the horizontal vector of the side branch under consideration. The variable HOR is calculated by:

$$\text{HOR} = \text{ALEN} \cdot \text{COS}(\text{ALT}_b) \tag{A10}$$

where ALEN is the length of the branch and ALT_b is the altitude of the branch above the horizon.

If the branch lies within the envelope described by $180 \pm \phi°$, the amount of the branch that is shaded is determined by considering the vertical geometry below in Figure A6. The length of the side branch shaded by the mainstem, Y, can be found from the equality:

$$\frac{Y}{\text{SIN } Z_s} = \frac{h - b}{\text{SIN } \gamma} \tag{A11}$$

where $\gamma = 180° - (Z_s + Z_b)$, the angle the branch makes with the shadowline, and b is the height at which the base of the side branch is attached to the mainstem. Substitution and rearrangement gives:

$$Y = \frac{\text{SIN } Z_s \ (h-b)}{\text{SIN}[180-(Z_s+Z_b)]} \tag{A12}$$

Thus, the length of a side branch shaded by the mainstem can be calculated if measurements of the branch and sun zenith (90° - Altitude),

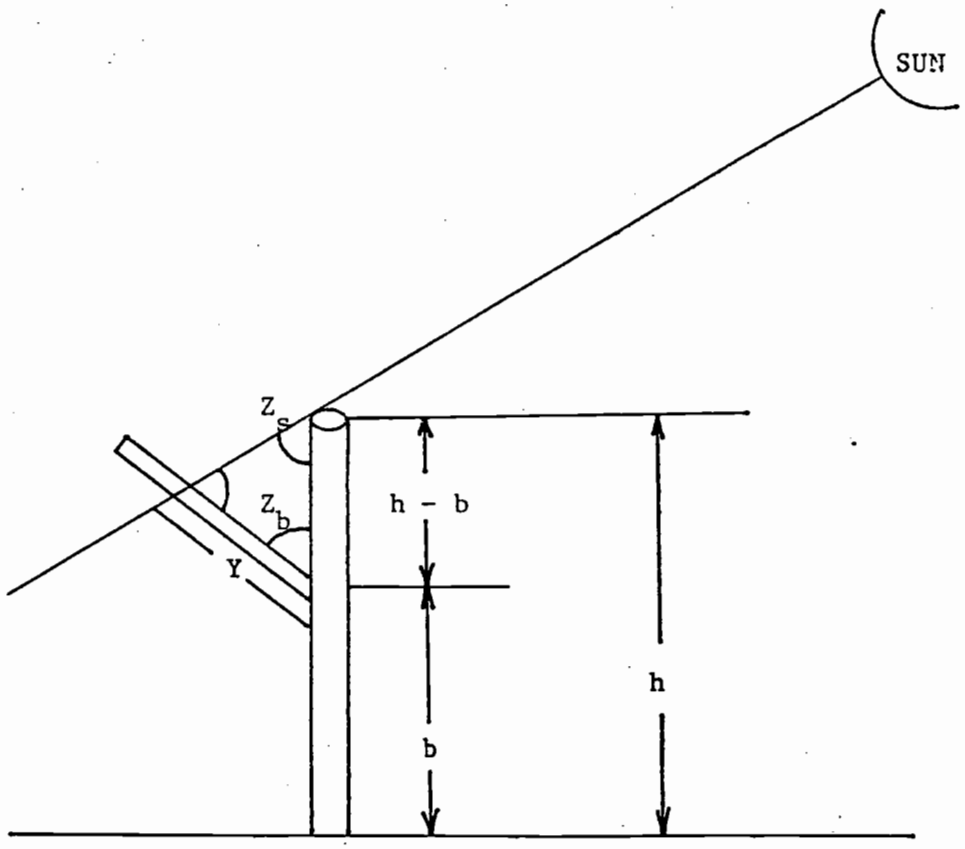

Figure A6. Vertical shading geometry of a sidebranch.

the height of the branch above the ground and the height of mainstem, are known.

The use of a cylindrical model greatly aids in simplifying the radiation geometry of the seedlings but is, obviously, an overestimation of the actual area receiving radiation. To determine the projected needle area (A_n) of a branch, photographs were taken of four branches, each at several different values of α, the angle between the sunline and the main axis of the branch. Examples of these photographs are shown in Figures A7-A8. A dot grid was used on each photograph to determine the projected needle area at that particular value of α. The factor A_n/LA, where LA is the one-sided leaf area of the branch, was plotted at various values of α for each of the four branches (Figure A9). The actual LA, as measured by a LICOR leaf area meter, was used for each except for the branch labelled D. This branch plotted very high but when the LA computed from the regression of needle dry weight against LA was used, it plotted right among the other three. A regression line was fitted to the four lines and used to determine the factor A_n/LA at any given value of α. This factor, multiplied by the one-sided LA of any particular branch, gave the projected needle area, A_n, of that branch at that value of α.

Direct and Diffuse Irradiance

Now that the area receiving shortwave radiation can be calculated for each branch at any time, the amount of radiation incident upon that area needs to be determined. The shortwave radiation received at a point on the earth's surface is made up of two components, that due to the solar beam, called the direct beam (S_o), and that due to

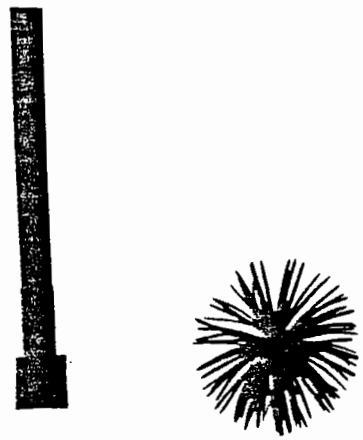

Figure A7. Photograph of branch at $\alpha = 0°$. Used in determination of A_n/LA.

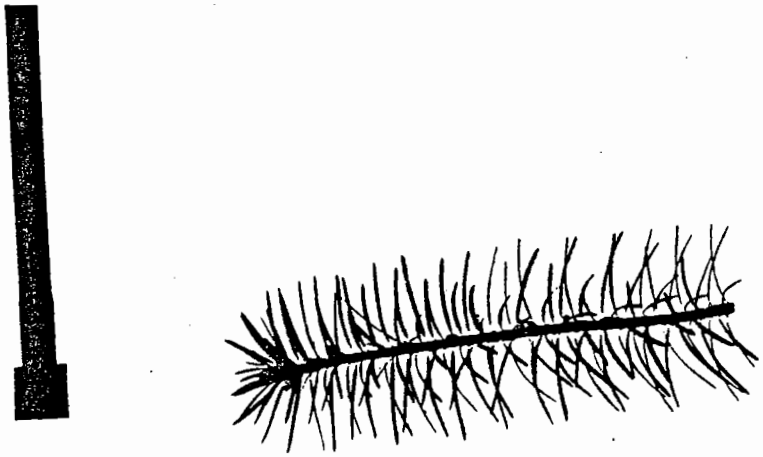

Figure A8. Photograph of branch at $\alpha = 90°$. Used in determination of A_n/LA.

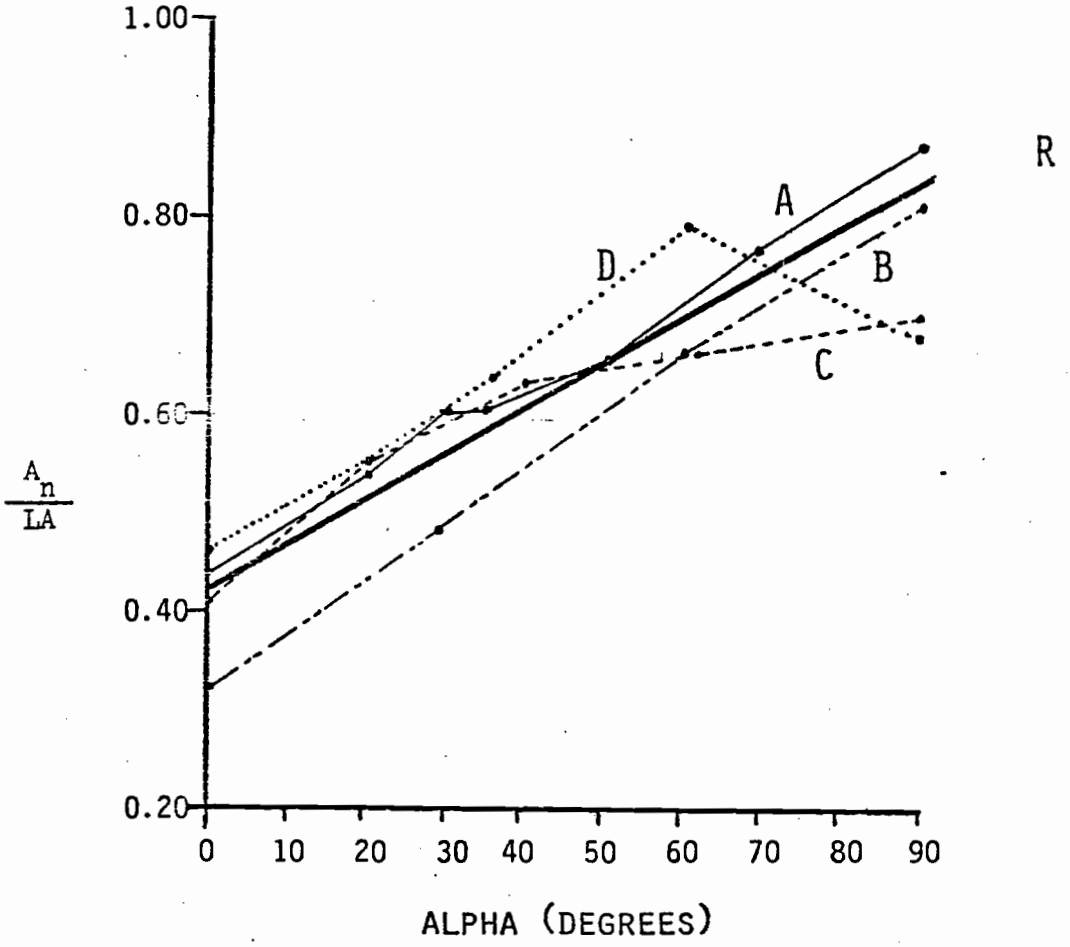

Figure A9. The factor A_n/LA versus the angle ALPHA (α) of the four branches (A, B, C, D) used to compute the regression line (R).

scattered radiation, called diffuse radiation (D). Combined, these two are often called the "incident solar" radiation, with the symbol $K\downarrow$.

Since the only radiation measurement made on site was that of solar radiation by a Moll-Gorcyznski pyranometer, a procedure was needed to estimate what part of the solar radiation the direct and diffuse components each made up. This is required because the direct beam is strongly a function of angles and, therefore, geometry is important in estimation of the direct beam flux to a seedling. The diffuse component, however, does not have an angular distribution and is received by the seedling over the entire area exposed to the sky.

Solar radiation can be expressed as a function of direct and diffuse by:

$$K\downarrow = S_o \cdot \cos Z_s + D \qquad \text{(A13)}$$

where $\cos Z_s$ corrects the direct beam back to the horizontally-oriented pyranometer. The diffuse beam, D, can be estimated by forming the ratio $D/K\downarrow$ for data gathered elsewhere. This ratio, however, has a parabolic shape over a diurnal period and would require a curve-fitting method in order to derive an equation for general use. Another method has been presented by Peterson and Dirmhirn (1981) and allows the use of a constant value throughout the day. This is done by forming a ratio between the diffuse and direct beam, D/S_o, which was found to change very little throughout the day. In order to estimate D, however, corresponding measurements of S_o are required. Since we did not have measurements of either D or S_o on our site, an

alternative method was used. This required using the constant formed by D/S_o in a method analogous to the Bowen ratio. Letting $D/S_o = d$, so that $D = d \cdot S_o$, and substituting this into equation A13 gives:

$$K\downarrow = S_o \cdot \cos Z_s + d\, S_o \tag{A14}$$

which can be rewritten as:

$$K\downarrow = S_o(d + \cos Z_s) \tag{A15}$$

An expression for S_o can thus be rewritten as:

$$S_o = \frac{K\downarrow}{(d + \cos Z_s)} \tag{A16}$$

The direct beam, S_o, is then calculated from measurements of $K\downarrow$, calculations from solar geometry, and calculations of d based on data for the Corvallis area. It follows that D is calculated by either $(D/S_o)(S_o)$, $K\downarrow - S_o$, or by a similar treatment as above where $S_o = D/d$ and substitution into A13 and rearrangement gives:

$$D = \frac{K\downarrow}{1 + \frac{\cos Z_s}{d}} \tag{A17}$$

Values of d were determined for D and S_o data from Corvallis (Rao et al., 1982). A value of 0.104 was used for d as determined from the Corvallis data.

In the clearcut there was no problem in using the incident solar radiation values directly in the preceding method to determine D and S_o. In the partial-cut, however, the shading by the tree canopy needs to be considered. When a tree element shades the pyranometer, the solar radiation will be composed entirely of the diffuse component. The ratio D/S_o, therefore, will not be a constant and the use of it during a shading "event" will overestimate S_o and underestimate D. To overcome this problem, values of D from the clearcut were used in the shelterwood and S_o was calculated from K↓ - D.

Now that values for A_n, S_o, and D can be obtained, the solar radiation incident upon a seedling can be calculated. The effective area for absorbing radiation from extended sources (non-directional radiation) was assumed to be equal to 0.9 times the total leaf area (2.3 LA) after Gates et al. (1965). Using the LA, the total area for receiving diffuse and longwave radiation would be $2.3 \cdot LA \cdot 0.9$. In addition, view factors for each type of surface seen by the seedling were determined. These are discussed later in the longwave radiation section.

Shadecard Shading

The shading by a shadecard will not begin until the sun has reached a point in azimuth equal to AZCARD + 90°. At this point, the shading by the shadecard can be calculated given the geometry shown in Figure A10. The distance a is calculated by:

$$a = \frac{x}{\text{TAN } Z_s} \qquad \text{(A18)}$$

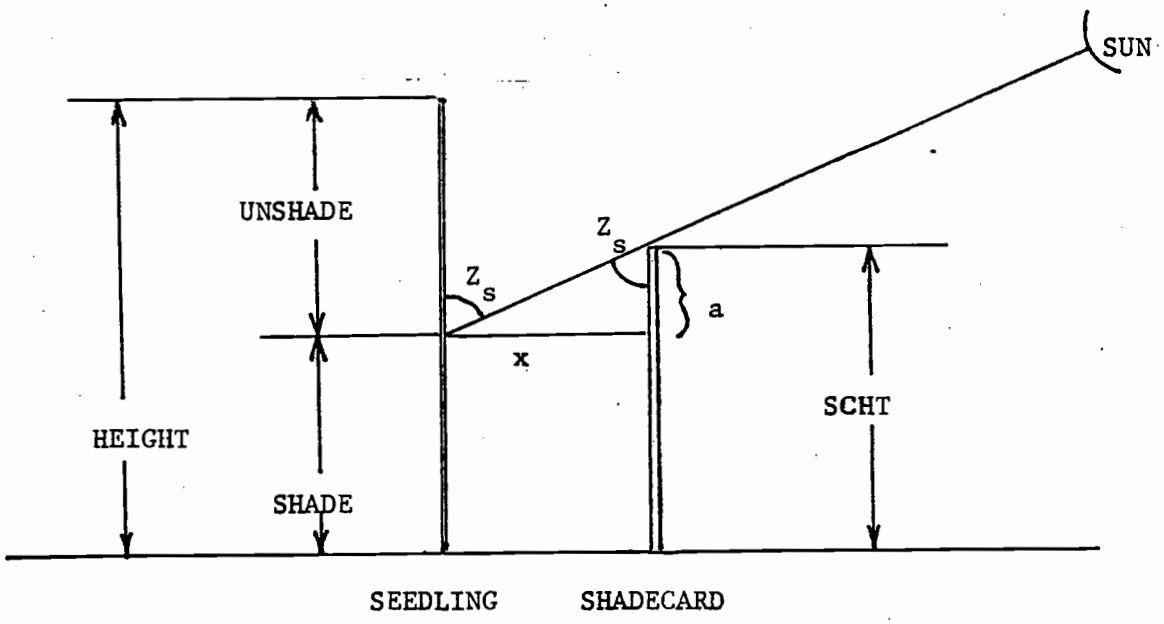

Figure A10. Vertical shading geometry of the shadecard upon a seedling.

where x is the distance from the stem to the card along the sunline, and Z_s is the zenith of the sun. The shaded portion of the seedling, SHADE, is:

$$\text{SHADE} = \text{SCHT} - a \text{ or } \text{SHADE} = \text{SCHT} - \frac{x}{\text{TAN } Z_s} \qquad \text{(A19)}$$

where SCHT is the shadecard height. The distance x is calculated given consideration of the horizontal geometry in Figure All. The distance x is calculated by:

$$x = \frac{m}{\text{COS } Q} \qquad \text{(A20)}$$

where m is the distance from the mainstem to the card along a line normal to the card which is also the line equal to 180° - AZCARD, Q is the angle between AZSUN and 180° - AZCARD, and x is as defined above. The two equations, A19 and A20, can now be combined to yield:

$$\text{SHADE} = \text{SCHT} - \frac{m}{\text{TAN } Z_s \text{ COS } Q} \qquad \text{(A21)}$$

Subsequently, the unshaded portion of the stem, UNSHADE, is:

$$\text{UNSHADE} = \text{HEIGHT} + \frac{m}{\text{TAN } Z_s \text{ COS } Q} - \text{SCHT} \qquad \text{(A22)}$$

where HEIGHT is the total height of the seedling.

Shortwave Exchange

Shortwave radiation received by a Douglas-fir needle surface can be either transmitted (t) through, reflected (r), or absorbed (a) by

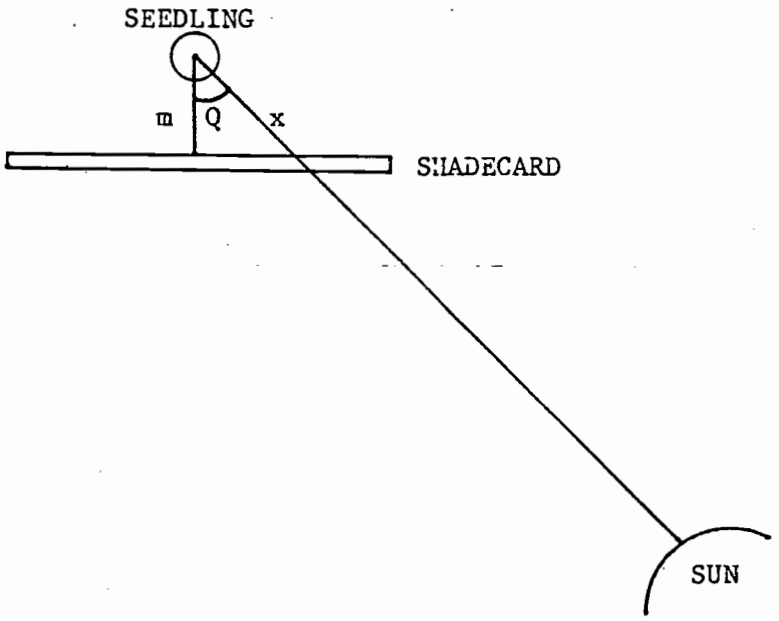

Figure A11. Horizontal shading geometry of the shadecard upon a seedling.

the needle. Woolley (1971) measured the spectral distribution of reflectivity for new and old needles of Douglas-fir. An integration of a wavenumber plot of his data gives an average reflectivity of 0.27 for new needles and 0.18 for old needles.

Since no transmissivity values for Douglas-fir were found in the literature, values for Sitka spruce [Picea sitchensis (Bong.) Carr.] were obtained from Norman and Jarvis (1974). They reported transmissivity for current year foliage between 0.02 and 0.05 for visible radiation (λ ~ 480 to 600 nm) and between 0.35 and 0.48 for near infrared radiation (λ ~ 700 to 1100 nm) depending upon height in the canopy. Transmissivity for old (1-year plus) foliage ranged from 0.01 to 0.02 for visible and 0.25 to 0.35 for near infrared. Using the shape of the transmissivity curve for Populus deltoides (Gates, 1965), a similar, artificial, curve of transmissivity versus wavenumber was plotted for Sitka spruce using the values given above by Norman and Jarvis (1974). An integration of these wavenumber plots gave values of $t = 0.18$ for new needles and $t = 0.12$ for old needles.

The absorptivity of Douglas-fir needles, a, is equal to 1-r-t. Given the above computed values for r and t, therefore, the absorptivity of shortwave radiation by new needles is 0.55 and by old needles is 0.70. The only published values found of absorptivities over all wavelengths for conifers was by Gates et al. (1965) for Pinus strobus and Thuja occidentalis. They assumed $t = 0$ and obtained a by measuring reflectivity alone ($a = 1-r$). Their values of 0.88 and 0.89 for a are probably overestimates (Jarvis et al., 1976) due to the assumption of zero transmissivity. For this study, $a = 0.70$ was used.

Longwave Exchange

Any object with a temperature above absolute zero (0 K or -273°C) emits radiant, longwave energy according to the Stefan-Boltzmann Law:

$$L = \varepsilon\sigma T^4 \qquad \text{(A23)}$$

where L is the emitted energy flux density (W/m^2), T is the temperature of the object in Kelvin, σ is the Stefan-Boltzmann constant (5.67×10^{-8} W/m^2K^4) and ε is the emissivity of the object, that fraction of radiant energy emitted by the object relative to a black body for which $\varepsilon = 1.00$.

A seedling will receive radiant, longwave energy from any object or surface that enters the "view" of the seedling. A seedling will also emit longwave radiation back to its surroundings by the relation described in equation A23. The net longwave, L*, energy received by a seedling can be described by the equation:

$$L^* = f_1\varepsilon_1\sigma T_1^4 + f_2\varepsilon_2\sigma T_2^4 + \ldots f_n\varepsilon_n\sigma T_n^4 - \varepsilon_\ell\sigma T_\ell^4 \qquad \text{(A24)}$$

where f_n is the "view factor," the fractional area of the seedling's hemispherical view, of the surface n, ε_n is the emissivity of n, and T_n is the surface temperature of n. The last term represents the outgoing longwave radiation from the seedling.

The values of f were determined from upward- and downward-facing fisheye photographs at each of the seedling locations. The view factors for each seedling are shown in Figure A12.

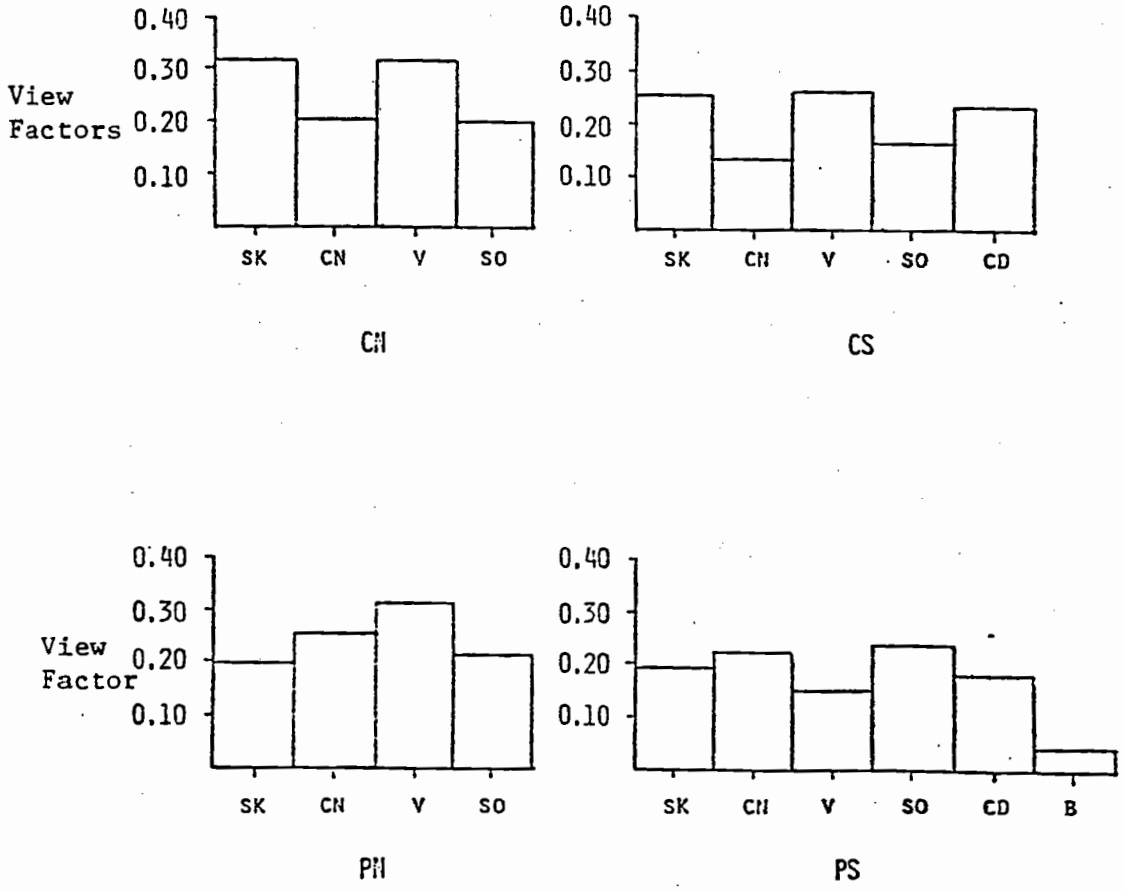

Figure A12. Longwave view factors of each of the four seedlings used in energy balance calculations. (SK = sky, CN = canopy, V = vegetation, SO = soil, CD = shadecard, B = black log.)

Given the view factors of each longwave-emitting surface seen by a seedling, the temperature of that surface needs to be estimated in order to calculate a longwave component from that surface. A separate technique was used for the estimation of longwave radiation from the sky.

The canopy, defined as that vegetation extending above the ground more than two feet, is assumed to be close to air temperature. The canopy temperature, therefore, was taken as the 2-m air temperature as recorded by the meteorological station. The temperatures of the near-ground vegetation, mostly grasses, and the shadecard were taken as the measured needle temperature of the seedling. The soil surface temperature was taken as the soil temperature at 0.1 cm which was calculated from a logarithmic extension of the five-depth soil temperature profile. The estimated soil surface temperature was most accurate during times of a stable profile (throughout midday) and least accurate during times when a "turnover" in the profile was occurring (sunrise and sunset). The temperature of the blackened log near seedling PS was estimated by the calculated soil surface temperature.

Since no measurements of atmospheric longwave radiation were made, and the estimation of sky temperatures is very difficult, an analytical frame-work was searched for which would allow the estimation of sky radiation based upon a measured variable. The best model found was a general relation developed between cloudless-sky atmospheric thermal radiation and screen-level air temperature that fit data from several, diverse, locations (Idso and Jackson, 1969). This relation is described by:

$$R = \sigma T^4 (1 - C \, EXP(-D(273 - T)^2)) \qquad (A25)$$

where R is the cloudless-sky atmospheric thermal radiation, T is the screen-level air temperature in Kelvin, σ is the Stefan-Boltzmann constant, C and D are coefficients determined by statistical analyses to have best fit values of 0.261 and 7.77×10^{-4}, respectively. Air temperature at 2-m, as recorded by the meteorological station, was used as the screen-level air temperature. Although it is recognized that general relations work best under "average" conditions and do not describe functional relationships (Monteith, 1973), the small variation in R and the small size of R with respect to shortwave radiation should allow the use of equation A25 without excessive error.

Before calculation of the longwave flux to a seedling, the effective surface area, A_{ce}, for absorbing or emitting longwave radiation had to be determined. Tibbals et al. (1964) used silver castings of blue spruce (Picea pungens Engelm.) and white fir [Abies concolor (Gord. & Glend.) Lindl.] and estimated A_{ce} at 0.88 and 0.94, respectively. Using the same method, Gates et al. (1965) estimated A_{ce} at 0.85 for ponderosa pine (Pinus ponderosa Dougl.). A value of 0.9 was used in this study for Douglas-fir.

APPENDIX B

```
C       PROGRAM SEEDRAD

C       This program calculates the net radiation loading upon a Douglas-fir seedling.
C       WRITTEN BY JAV 3/31/82

        REAL KNET, KIN, KOUT, LNET, LIN, LOUT
        DIMENSION ID(50), AZBR(50), ZBR(50), GLOBAL(50), TLEAF(50), NAME5(10)
        DIMENSION ALEN(50), ANL(50), BASE(50), ALAI(50), ANEEDLE(50), NAME(10)
        DIMENSION NAME1(10), SGLOBAL(50), AIRTEMP(50), NAME2(10), NAME3(10), SAIRTEMP(5
        DIMENSION NAME4(10), TSURF(50), NAME6(10)

        ACCEPT 'NUMBER OF AVERAGING PERIODS PER DAY >', N
        ACCEPT 'JULIAN DATE DESIRED >', NDATE
        ACCEPT 'INPUT LATITUDE OF SITE >', ALAT
        ACCEPT 'INPUT LONGITUDE OF SITE >', ALONG

        PI=3.141592654
        STEF=5.6697E-08

C       Input values of azimuth, zenith, length, radius (average needle length),
C       and height above ground for each branch on seedling

        LUN=LUNIO(1,NAME)
        READ(LUN,25,END=31) (ID(J),AZBR(J),ZBR(J),ALEN(J),ANL(J),BASE(J),ALAI(J),J=1,30
25      FORMAT(I2,F6.1,2F5.1,F5.2,F5.1,F5.1)
31      NBR=J

        ACCEPT ' ENTER 0 IF CLEARCUT, 1 IF SHELTERWOOD >', IDEC
        TYPE "ENTER CLEARCUT METFILE FOR DAY"
        LUN1=LUNIO(1,NAME1)

        IF(IDEC.EQ.0) GO TO 34
        TYPE "ENTER SHELTERWOOD METFILE FOR DAY"
        LUN2=LUNIO(1,NAME2)

        READ(LUN2,36) BURP
        READ(LUN2,37) (SAIRTEMP(K), SGLOBAL(K), K=1,47)
34      READ(LUN1,36) TURKEY
        READ(LUN1,37) (AIRTEMP(K), GLOBAL(K), K=1,47)

        CALL CLOSE(LUN,IERR)
        CALL CLOSE(LUN1,IERR)

C       Enter the viewfactor file for the seedling.  The viewfactors are the
C       fractions of the hemispherical view "seen" by the various surfaces
C       around the seedling which emit longwave radiation to that seedling.

        TYPE "***VIEWFACTOR FILE FOR SEEDLING***"
        LUN3=LUNIO(1,NAME3)
        READ(LUN3,39) VFSKY, VFCAN, VFCARD, VFLOG, VFSOIL, VFVEG, AZCARD, ZCARD,
     /  SCHT, DIST
```

```
C       Enter the soil surface temperature file representative of that
C       seedling.  This will be used to calculate the longwave flux to the seedling
C       from the soil.

        TYPE "ENTER TSURF FILENAME"
        LUN4=LUNIO(1,NAME4)
        READ(LUN4,77) DUM1,(TSURF(K),K=1,47)

        ACCEPT "IF C51 OR S49 ENTER 0, IF C53 OR S50 ENTER 1>", ICY

C       Enter the leaf temperature file for the seedling.

        TYPE "ENTER TLEAF FILENAME"
        LUN5=LUNIO(1,NAME5)
        IF(ICY.EQ.1) GO TO 23
        READ(LUN5,81) DUM2, (TLEAF(K),K=1,47)
        GO TO 26
23      READ(LUN5,82) DUM2, (TLEAF(K),K=1,47)

26      TYPE"***OUTPUT FILENAME***"
        LUN6=LUNIO(2,NAME6)

36      FORMAT(39X,F7.3,35X)
37      FORMAT(15X,F8.3,16X,F7.3,35X)
39      FORMAT(6F5.2,4F5.1)
77      FORMAT(5X,F8.3,8X,/)
81      FORMAT(13X,F7.3,/)
82      FORMAT(55X,F7.3,/)

C       Calculate the total height of the seedling.  The data files are set up
C       up such that the height of the mainstem is in ALEN(1) and the height of
C       the terminal branch is in ALEN(2).  The total height is later used in
C       the subroutine SHADE and in calculating the shading by the shadecard.

        HEIGHT=ALEN(1)+ALEN(2)
        APER=FLOAT(N)

C       Sum the leaf area (LA) for the seedling.

        SUMLA=0.
        DO 40 L=1,NBR
                SUMLA=SUMLA+ALA(L)
40      CONTINUE

C ***   SHORTWAVE RADIATION  ***
C       This section computes the net shortwave radiation balance of a
C       seedling.  It uses a subroutine, ALMANAC, to determine the solar
C       position at half-hour intervals during the day.

        DO 121 ITIME=1,N
                TIME=FLOAT(ITIME*24)/APER
                CALL ALMANAC(NDATE,ALAT,ALONG,TIME,ALT,AZSUN)
                ZSUN=90.00-ALT
```

```
                SUM=0
                DIRLOAD=0
                DIFFLOAD=0
                REFLOAD=0

C       For each time period, compute the direct and diffuse components of the
C       global irradiance.  Global is defined as direct + diffuse solar radiation.

                DIRECT=GLOBAL(ITIME)/(0.104+COS(ZSUN*PI/180.))
                DIFFUSE=0.104*DIRECT

                IF(IDEC.EQ.0) GO TO 44
                DIRECT=SGLOBAL(ITIME)-DIFFUSE
                DIRECT=DIRECT/COS(ZSUN*PI/180.)
                GLOBAL(ITIME)=SGLOBAL(ITIME)

C       For each branch, compute the angle, ALPHA, that is formed by the
C       sun's rays and the branch.

44              DO 51 IBR=1,NBR
                ANGLE=ALPHA(AZSUN,ZSUN,AZBR(IBR),ZBR(IBR))
                IF (ANGLE.GT.90) ANGLE=180-ANGLE

C       Compute the factor (FACTOR) by which LA is reduced as a function of ALPHA.
C       This is derived from the regression of ALPHA against needle areas
C       measured from photographs of branches.
C       Compute the projected needle area (ANEEDLE) for the branch.

                FACTOR=0.42695+0.00456*ANGLE
                ANEEDLE(IBR)=FACTOR*ALA(IBR)

C       Compute fraction of branch shaded by the mainstem (1 - CORRECT).
C         This is used to correct the projected needle area as a result of shading.

                CALL SHADE(AZSUN,AZBR(IBR),ALEN(IBR),ANL(1),ZBR(IBR),ZSUN,BASE(IBR),
     /          HEIGHT,SHADED)
                SHADED=SHADED*0.5
                CORRECT=1-(SHADED/ALEN(IBR))
                ANEEDLE(IBR)=ANEEDLE(IBR)*CORRECT

C       Sum the projected needle areas of the branches for each time interval.

                SUM=SUM+ANEEDLE(IBR)

51              CONTINUE

C       Compute the direct solar beam incident to the seedling.  Calculate the
C       the amount of stem shaded by the shadecard and reduce SUM by this amount.
C       If the seedling does not have a shadecard, this will result in SCHT=0,
C       thus skipping the shading computation.

                ANGLE2=ALPHA(AZSUN,ZSUN,AZCARD,ZCARD)
                IF(SCHT.EQ.0.) GO TO 57
                IF(ANGLE2.LE.90.) GO TO 57
```

```
                ANG1=ABS(180.+AZCARD-AZSUN)
                HENRY=DIST/(TAN(ZSUN*PI/180.)*COS(ANG1*PI/180.))
                IF(HENRY.GT.SCHT) HENRY=SCHT
                UNSHADE=HEIGHT+HENRY-SCHT
                SUM=UNSHADE*SUM/HEIGHT

57              DIRLOAD=DIRECT*SUM


C       Compute the diffuse and reflected diffuse beam incident to
C       the seedling.

                ALFRED=0.15*VFCAN+0.2*VFSOIL+0.2*VFVEG+0.4*VFCARD+VFSKY
                DIFFLOAD=DIFFUSE*0.9*SUMLAI*2.3*ALFRED

C       Compute the reflected direct beam incident to the seedling.

                ANG=ANGLE2
                IF(ANGLE2.GT.90.) ANG=90.
                BUZZ=0.2*VFSOIL+0.4*VFCARD*COS(ANG*PI/180.)
                REFLOAD=DIRECT*0.9*SUMLAI*2.3*BUZZ

C       Compute the total shortwave radiation incident to the seedling.
C       If the global radiation is less than 0, set the incoming shortwave
C       equal to 0.

                KIN=(DIRLOAD+DIFFLOAD+REFLOAD)/10.
                CHECK2=GLOBAL(ITIME)
                IF(CHECK2.LE.0.) KIN=0.

C       Compute outgoing solar radiation as 1-abs. or 30% for these Douglas-fir
C       needles.  Compute the net solar radiation (KNET).

        KOUT=0.3*KIN
        KNET=KIN-KOUT


C ***   LONGWAVE RADIATION  ***
C       This section computes the longwave radiation loading onto the seedling.
C       It requires the temperatures, emissivities, and view factors for the
C       surfaces "seen" by the seedling.


C       Sky radiation is estimated from an empirical relation derived by
C       Idso and Jackson (1969).

        C=0.261
        D=7.77E-4
        ATIK=AIRTEMP(ITIME)+273.16
        CARRY=STEF*ATIK**4.0
        SKYRAD=CARRY-(C*CARRY)/(EXP(D*(AIRTEMP(ITIME)**2.0)))
        SKYLONG=SKYRAD*VFSKY

C       Canopy radiation is estimated from the Stefan-Boltzmann Law
```

```
C       using the air temperature at 2-m as the "canopy" temperature.
C       For the clearcut, the variable ATIK from above is used since it
C       represents the 2-m air temperature.  For the shelterwood,
C       the air temperature from the shelterwood has to be used.

        IF(IDEC.EQ.1) ATIK=SAIRTEMP(ITIME)+273.16
        CANRAD=0.98*STEF*ATIK**4.0
        CANLONG=VFCAN*CANRAD

C       Soil longwave radiation is estimated from the Stefan-Boltzmann Law
C       using the calculated soil temperature at 0.1 cm as the "surface"
C       temperature.  This value is read in from TSURF files.

        TSIK=TSURF(ITIME)+273.16
        SOILRAD=0.95*STEF*TSIK**4.
        SOILONG=VFSOIL*SOILRAD

C       The radiation from the black log around S50 is also estimated
C       from the Stefan-Boltzmann Law using the soil "surface" temperature.

        BLOGRAD=STEF*TSIK**4.
        BLOGLONG=VFLOG*BLOGRAD

C       The longwave radiation from the shadecard and vegetation is calculated
C       from the Stefan-Boltzmann Law using the temperature of the needle.

        TIK=TLEAF(ITIME)+273.16
        VCRAD=0.97*STEF*TIK**4.
        VCLONG=(VFCARD+VFVEG)*VCRAD

C       Total the longwave radiation components.  The sum has to be divided
C       by 10,000 in order to correct m2 to cm2.

        RADLONG=SKYLONG+CANLONG+SOILONG+BLOGLONG+VCLONG
        LIN=RADLONG*0.9*SUMLAI*2.3*0.0001

C       Compute the outgoing longwave by the Stefan-Boltzmann Law
C       using the needle temperature.  Compute the net longwave (LNET).  Compute
C       the net radiation balance (QSTAR) of the seedling.

        LORAD=0.97*STEF*TIK**4.
        LOUT=LORAD*0.9*SUMLAI*2.3*0.0001
        LNET=LIN-LOUT
        QSTAR=KNET+LNET

        WRITE(LUN6,88) TIME, KIN, KNET, LIN, LNET, QSTAR
88      FORMAT(2X,F5.2,5(3X,F7.2))

121     CONTINUE
```

```
CALL EXITV
CALL CLOSE(LUN2,IERR)
CALL CLOSE(LUN3,IERR)
CALL CLOSE(LUN4,IERR)
CALL CLOSE(LUN5,IERR)
CALL CLOSE(LUN6,IERR)
END
```

```
C       SUBROUTINE ALMANAC

C       This subroutine calculates the solar altitude and
C       azimuth for time increments throughout the day.
C       The Julian date, latitude, longitude, and time of
C       interest are called from the program accessing almanac.

C       WRITTEN BY JAV 3/31/82

C       DEC = SOLAR DECLINATION
C       AZSUN = SOLAR AZIMUTH
C       ALT = SOLAR ALTITUDE
C       SUNTIM = SOLAR TIME
C       HANG = HOUR ANGLE
C       EQTIM = EQUATION OF TIME

        SUBROUTINE ALMANAC (NDATE,ALAT,ALONG,TIME,ALT,AZSUN)

        PI=3.141592654

        DEC=0.40928*SIN(4.88883+0.01721*NDATE)

        EQTIM=(0.7*SIN(-0.986*NDATE)+SIN(-1.97*NDATE-13.78))/6

        SUNTIM=TIME+EQTIM+(120.0-ALONG)/15

        HANG=15*(SUNTIM-12.0)

C       CONVERT ANGLES TO RADIANS.
        HANG=HANG*PI/180
        ALAT=ALAT*PI/180

C       DETERMINE SOLAR ALTITUDE
        TSIN=SIN(ALAT)*SIN(DEC)+COS(ALAT)*COS(DEC)*COS(HANG)
        ALT=ASIN(TSIN)

C       COMPUTE SOLAR AZIMUTH
        TCOS=(SIN(DEC)*COS(ALAT)-COS(DEC)*SIN(ALAT)*COS(HANG))/COS(ALT)
        AZSUN=ACOS(TCOS)

C       CONVERT EVERYTHING BACK TO DEGREES
        AZSUN=AZSUN*180/PI
        ALT=ALT*180/PI
        ALAT=ALAT*180/PI

        IF(SUNTIM.LE.12.00) GO TO 28
        AZSUN=360.00-AZSUN

28      RETURN
        END
```

```
C       SUBROUTINE FUNCTION ASIN
C       THIS SUBROUTINE CALCULATES THE INVERSE SINE FUNCTION
C       WRITTEN BY ELM 3/29/82

        FUNCTION ASIN(VAR)

        I=0
        VAR2=VAR*VAR
        ASIN=VAR
        COEF=VAR
10      I=I+2
        COEF=COEF*VAR2*FLOAT(I-1)/FLOAT(I)
        TERM=COEF/FLOAT(I+1)
        ASIN=ASIN+TERM
        FRAC=ABS(TERM/ASIN)
        IF(FRAC.GT.0.00001) GO TO 10
        RETURN
        END



C       SUBROUTINE FUNCTION ACOS
C       THIS SUBROUTINE CALCULATES THE INVERSE COSINE FUNCTION
C       WRITTEN BY JAV 3/29/82

        FUNCTION ACOS(VAR)

        ACOS=(3.141592654/2)-ASIN(VAR)
        RETURN
        END
```

```
C       SUBROUTINE FUNCTION ALPHA

C       This program determines alpha, the angle between a branch
C       and the sunline.
C       WRITTEN BY JAV 3/31/82

        FUNCTION ALPHA(AZSUN,ZSUN,AZBR,ZBR)

        PI=3.141592654

        IF (AZBR.EQ.0.0) GO TO 11

C       Convert input angles to radians.

        AZSUN=AZSUN*PI/180
        ZSUN=ZSUN*PI/180
        AZBR=AZBR*PI/180
        ZBR=ZBR*PI/180

C       Determine alpha

        TCOS=SIN(ZSUN)*SIN(ZBR)*COS(AZSUN-AZBR)+COS(ZSUN)*COS(ZBR)
        ALPHA=ACOS(TCOS)

C       Convert input angles back to degrees.

        AZSUN=AZSUN*180/PI
        ZSUN=ZSUN*180/PI
        AZBR=AZBR*180/PI
        ZBR=ZBR*180/PI
        GO TO 21

11      ALPHA=ABS(ZBR-ZSUN)
        ALPHA=ALPHA*PI/180

21      RETURN
        END
```

```
C       Subroutine SHADE

C       This subroutine calculates the amount of branch length shaded by
C       the main stem.  First, it determines if the branch is shaded.
C       Then it calculates the amount of the branch shaded.  This value
C       is returned to the main program in the value of SHADED.

C       Written by JAV 4/28/82

        SUBROUTINE SHADE(AZSUN,AZBR,ALEN,ANL,ZBR,ZSUN,BASE,HEIGHT,SHADED)

        PI=3.141592654

C       Make an initial guess as to whether branch is shaded by the main stem.
C       If the branch azimuth is not between 160 and 200 degrees opposite
C       the sun azimuth, return to main program without further calculations.

        DIFF=ABS(AZSUN-AZBR)
        IF(DIFF.LT.160) GO TO 47
        IF(DIFF.GT.200) GO TO 47

C       Compute altitude angle of branch from the zenith angle.  Convert
C       altitude to radians.

        ALTBR=90-ZBR
        ALTBR=ALTBR*PI/180

C       Compute horizontal vector of branch.  This is then used to compute
C       THETA, half of the angle that subtends the shadow of the mainstem.
C       Convert THETA to degrees.

        HORIZ=ALEN*COS(ALTBR)
        THETA=ATAN(ANL/HORIZ)
        THETA=THETA*180/PI

C       Determine if the branch is shaded by the mainstem.
C       To be shaded, the azimuth of the branch must be within THETA degrees
C       of being 180 degrees opposite of the sun's azimuth.

        IF(DIF.GT.180) GO TO 21
        CHECK=180-THETA
        IF(DIFF.GE.CHECK) GO TO 31
        GO TO 47

21      CHECK=180+THETA
        IF(DIFF.LE.CHECK) GO TO 31
        GO TO 47

C       Calculates the length of branch shaded be the sun.  If calculated
C       value of SHADED is larger than the branch length, set SHADED equal
C       to the branch length.
```

```
31      RHO=180-ZSUN-ZBR
        RHO=RHO*PI/180
        DUMMY=ZSUN*PI/180
        SHADED=(SIN(DUMMY)*(HEIGHT-BASE))/SIN(RHO)
        IF(SHADED.GT.ALEN) SHADED=ALEN
        GO TO 51

47      SHADED=0
51      RETURN
        END
```

APPENDIX C

```
C       PROGRAM HEATDUMP.FR

C       This program takes the net radiation of a seedling and partitions
C       it into the two predominant modes of heat dissipation, latent heat and
C       convective (sensible) heat, using measurements made in the field.
C       Written by JAV 8/23/82 on the occasion of the 2nd anniversary of his
C       marriage to Jeanne Marie Hunsucker.

        REAL LATHEAT
        DIMENSION NAME(10), NAME1(10), NAME2(10), NAME3(10)
        DIMENSION QSTAR(50), TDEW(50), WIND(50), TLEAF(50), DELTA(50), RSTOM(50)
        DIMENSION TAIR2M(50), TDEW2M(50)

        TYPE "***SEEDLING RADIATION FILE***"
        LUN=LUNIO(1,NAME)
        READ(LUN,17) (QSTAR(K),K=1,48)

        TYPE "***METFILE***"
        LUN1=LUNIO(1,NAME1)
        READ(LUN1,19) (TAIR2M(K), TDEW2M(K), TDEW(K), WIND(K), K=1,48)

        TYPE "***TLEAF FILE***"
        LUN2=LUNIO(1,NAME2)
        ACCEPT "IF C51 OR S49 ENTER 0, IF C53 OR S50 ENTER 1>", ICY
        IF(ICY.EQ.1) GO TO 13
        READ(LUN2,21) (TLEAF(K), DELTA(K), K=1,48)
        GO TO 15
13      READ(LUN2,23) (TLEAF(K), DELTA(K), K=1,48)

15      ACCEPT "ENTER SUM OF THE LA>", SUMLA
        SUMLA=SUMLA*0.0001

        TYPE "***STOMATAL RESISTANCE FILE***"
        LUN3=LUNIO(1,NAME3)
        READ(LUN3,25) (RSTOM(K),K=1,48)

17      FORMAT(46X,F10.2)
19      FORMAT(15X,3F8.3,28X,F7.3)
21      FORMAT(6X,F7.3,7X,F7.3,/)
23      FORMAT(48X,F7.3,7X,F7.3,/)
25      FORMAT(12F6.0)
        CALL CLOSE(LUN,IERR)
        CALL CLOSE(LUN1,IERR)
        CALL CLOSE(LUN2,IERR)
        CALL CLOSE(LUN3,IERR)

        DO 80 J=1,48
                TIME=FLOAT(J)*0.5-0.5
```

```
C  ***  VAPOR DENSITY DEFICIT ***
C       Calculates the vapor density deficit of the air around the seedling
C       and the saturated vapor density of the needle.  Teten's approximation
C       is used with the dewpoint temperature and the needle temperature.

        UTAH=17.27*TLEAF(J)/(237.3+TLEAF(J))
        VDLEAF=(1323.*EXP(UTAH))/(TLEAF(J)+273.16)

        COLO=17.27*TDEW(J)/(237.3+TDEW(J))
        VDAIR=(1323.*EXP(COLO))/(TDEW(J)+273.16)

        VDDEF=VDLEAF-VDAIR

C   *** LATENT HEAT CALCULATION ***
C       Calculates the latent heat dissipation in W/m2 by using the vapor density
C       deficit and the stomatal resistance.  Also calculates total water
C       use of the seedling for the half-hour period.  Units are in
C       cm3/period.

        RSTOM(J)=RSTOM(J)*100.
        EVAP=VDDEF/RSTOM(J)
        WATUSE=EVAP*SUMLAI*1800.
        LATHEAT=LAMBDA*EVAP

C  ***  CONVECTIVE HEAT EXCHANGE  ***
C       Estimates the amount of heat lost by convective (sensible) heat
C       transfer by use of the equation for RHEAT from Campbell (1977).
C       Convective heat, H, is also calculated by difference: Q* - LE.

        UBAR=WIND(J)*0.3
        RHEAT=307.*SQRT(0.001/UBAR)
        SENSHT=1200.*DELTA(J)/RHEAT

        RADNET=QSTAR(J)/SUMLAI
        H=RADNET-LATHEAT

C  ***  BOWEN RATIO  ***
C       This is the Bowen ratio of each individual seedling.

        BOWEN=H/LATHEAT

        WRITE(12,41) TIME, WATUSE, LATHEAT, SENSHT, H, RADNET, BOWEN
41      FORMAT(1X,F5.2,9F9.2)

80      CONTINUE
        END
```

APPENDIX D

Error in Measurements

The analysis of error follows that of Scarborough (1966) as outlined by Holbo (1973) and Fritschen and Gay (1979). The error in the energy balance terms, all indirect measurements, must be calculated from the error in the equipment and methods used to calculate the energy balance terms. An indirect measurement, M, can be described as a function of its component variables, X_i, as:

$$M = f(X_1, X_2, X_3, \ldots, X_n) \tag{1}$$

Each of these variables has an absolute error ΔX such that:

$$M + \Delta M = f(X_1 + \Delta X_1, X_2 + \Delta X_2, \ldots, X_n + \Delta X_n) \tag{2}$$

Expanding the right side by Taylor's theorem, ignoring the small terms, and subtracting from equation 1 gives:

$$\Delta M = \Delta X_1 \frac{\partial M}{\partial X_1} + \Delta X_2 \frac{\partial M}{\partial X_2} \ldots + \Delta X_n \frac{\partial M}{\partial X_n} \tag{3}$$

This allows the calculation of the absolute error in M from the absolute error in each component variable and the sensitivity of M to each component variable. This is the error resulting from the worst possible case. If the errors are considered to be normally distributed, there is the probability that the errors in the variable will compensate each other to some extent. In this case, the probable

error in M, δM, is estimated by combining individual probable errors, δX, through least squares:

$$\delta M = [(\delta X_1 \frac{\partial M}{\partial X_1})^2 + (\delta X_2 \frac{\partial M}{\partial X_2})^2 \ldots + (\delta X_n \frac{\partial M}{\partial X_n})^2]^{1/2} \qquad (4)$$

This probable error estimate will be smaller than the absolute error calculated from equation 3. Because some mutual compensation of individual variable errors is expected, the probable error will be calculated for each of the energy balance terms.

Error in Latent Heat Flux

The latent heat flux, LE, was given earlier by:

$$LE = \lambda \frac{\rho^1 - \rho}{r_s} \qquad (5)$$

The probable error in LE can be written as:

$$\delta LE = [(\delta \rho^1 \frac{\partial LE}{\partial \rho^1})^2 + (\delta \rho \frac{\partial LE}{\partial \rho})^2 + (\delta r_s \frac{\partial LE}{\partial r_s})^2]^{1/2} \qquad (6)$$

with λ, the latent heat of vaporization, treated as a constant. Each of the right hand terms in equation 5 can be broken down further into their component parts. The vapor densities are both functions of temperature and the uncertainty can be written:

$$\delta \rho = \delta T \frac{\partial \rho}{\partial T} \qquad (7)$$

The uncertainty of the temperature measurements, δT, was $\pm$ 1°C. The vapor density was calculated using Teten's Approximation:

$$\rho = \frac{1325 \exp(17.27T/237.3+T)}{273.16 + T} \tag{8}$$

which, when differentiated with respect to T, gives:

$$\frac{\partial \rho}{\partial T} = \frac{1325 \exp(17.27T/237.3+T)\{(273.16+T) \left[\frac{4098.17}{(237.3+T)^2} - 1\right]\}}{(273.16+T)^2} \tag{9}$$

The differentiation of LE with respect to ρ, $\partial LE/\partial \rho$, is simply λ/r_s. Thus, the first two terms on the right side of equation 5 can be combined to give:

$$\delta LE = 2(\delta T) \frac{\partial \rho}{\partial T} \frac{\lambda}{r_s} \tag{10}$$

with $\partial \rho/\partial T$ given by equation 8. The units are in W/m^2. For the third term in equation 5, r_s is determined by a null balance diffusion porometer which has a functional relationship of:

$$r_s = \left(\frac{100}{RH} - 1\right) \frac{A}{F} \tag{11}$$

where RH is the null balance relative humidity of the chamber the sample is placed in, A is the leaf area of the sample and F is the nitrogen gas flow rate (Beardsell et al., 1972). The error in r_s, therefore, is a result of the error in RH, A, and F. This can be written:

$$\delta r_s = [(\delta RH \frac{\partial r_s}{\partial RH})^2 + (\delta A \frac{\partial r_s}{\partial A})^2 + (\delta F \frac{\partial r_s}{\partial F})^2]^{1/2} \quad (12)$$

Specifications for the Interface porometer were used to determine δRH and δF. Specifications for the LI-3000 leaf area meter (Li-Cor, Inc.; Lincoln, Nebraska) suggest an error in A on the order of 5%. An analysis of δr_s resulted in errors ranging 10% to 29%. Since the high values of r_s tended to occur under conditions of RH and F that were not realized during the field study, a more conservative value of 15% was chosen to represent δr_s. Equation 12, along with $\partial LE/\partial r_s$ gives the third term in equation 6. This equation can now be written:

$$\partial LE = \{[2(1°C) \frac{\lambda}{r_s} (\text{Eqn. } 8)]^2 + [(0.15\ r_s) \frac{\lambda(\rho^1 - \rho)}{r_s^2}]^2\}^{1/2} \quad (13)$$

using the derived expressions and values from above.

Calculations of error are shown in Table D1 for several sets of values that are in the range found in field measurements. The relative probable error, δLE/LE, was 15%. This value is the same as the 15% error in r_s. This is not surprising since the error in r_s (last term in equation 6) makes up about 95% of the total error in LE.

Error in Net Radiation

The net radiation, Q*, of a seedling was written earlier as:

$$Q^* = K\downarrow - K\uparrow + L\downarrow - L\uparrow \quad (14)$$

which is the summation of incoming and outgoing radiant energy fluxes. The probable error in Q* can be written:

$$\delta Q^* = [(\delta K\downarrow \frac{\delta Q^*}{\delta K\downarrow})^2 + (\delta K\uparrow \frac{\delta Q^*}{\delta K\uparrow})^2 + (\delta L\downarrow \frac{\delta Q^*}{\delta L\downarrow})^2 + (L\uparrow \frac{\delta Q^*}{\delta L\uparrow})^2]^{1/2} \quad (15)$$

Knowing that $K\uparrow = aK\downarrow$, where a is the albedo of the seedling leaf surface (a constant), the first two terms on the right side of equation 14 can be combined into $2(\delta K)(\partial Q^*/\partial K)$.

The functional relationship for K can be described by:

$$K = 0.65\ DIR + 0.36\ DIFF + 0.09\ REF \quad (16)$$

where DIR is the direct solar radiation, DIFF is diffuse solar radiation, and REF is the reflected solar radiation. The error in K is:

$$\delta K = \delta DIR(0.65) + \delta DIFF(0.36) + \delta REF(0.09) \quad (17)$$

Since DIFF = 0.104·DIR and REF = albedo·DIR, the uncertainty in those two will be $\delta DIR(\partial DIFF/\partial DIR)$ and $\delta DIR(\partial REF/\partial DIR)$, respectively. With the albedo = 0.1, this allows the rewriting of equation 17 as:

$$\delta K = (0.65)(\delta DIR) + (0.04)(\delta DIR) + (0.01)(\delta DIR) \quad (18)$$

revealing that δK only depends upon δDIR. The functional relationship for DIR is:

$$DIR = \frac{GLOBAL}{0.104 + \cos Z_s} \quad (19)$$

with GLOBAL the global solar radiation as measured by the Moll-Gorczynski pyranometer and Z_s is the sun zenith angle. The error in DIR, δDIR, is equal to δGLOBAL(∂DIR/∂GLOBAL). This is equal to:

$$\delta DIR = (\delta V)(\partial GLOBAL/\partial V)\left(\frac{1}{0.104 + \cos Z_s}\right) \quad (20)$$

where δV is the accuracy of the digital voltmeter which records the pyranometer signal, and ∂GLOBAL/∂V is simply 1/c, where c is the calibration factor of the pyranometer in mV per W/m^2. These were evaluated as δV = 0.2% of the millivolt signal (Campbell Scientific, 197) and c = 0.011 $mV/W/m^2$ for the pyranometer (from calibration tests). Combining equations 18 and 20 and rewriting terms gives:

$$\delta K = (0.7)(\delta V)(1/c)\left(\frac{1}{0.104 + \cos Z_s}\right) \quad (21)$$

The functional relationship for L↓ is:

$$L\downarrow = 0.9(SKY + CAN + SOIL + BLOG + VC) \quad (22)$$

with

$$\delta L\downarrow = 0.9[(\delta SKY^2 + \delta CAN^2 + \delta SOIL^2 + \delta BLOG^2 + \delta VC^2)^{1/2}] \quad (23)$$

where SKY is the longwave radiation from the sky, CAN is from the canopy, SOIL is from the soil surface, BLOG is from a black log (around PS only), and VC is from surrounding vegetation and the shade-card, if there is one. Evaluation of each of these components given

their functional relationships (see SEEDRAD program in Appendix B) and representative values of environmental temperatures (from which they were calculated, see Appendix A), the respective errors are:

$$\begin{aligned} \delta SKY &= 3.33 \text{ W/m}^2 \\ \delta CAN &= 1.24 \text{ W/m}^2 \\ \delta SOIL &= 6.00 \text{ W/m}^2 \\ \delta BLOG &= 1.60 \text{ W/m}^2 \\ \delta VC &= 2.45 \text{ W/m}^2 \end{aligned}$$

which, when substituted into equation 23 results in:

$$\delta L\downarrow = 0.9(7.56 \text{ W/m}^2) = 6.8 \text{ W/m}^2 \tag{24}$$

This value will be somewhat constant since the environmental temperatures do not change much in the temperature scale (Kelvin) required by the Stefan-Boltzmann equation.

The outgoing longwave radiant flux, $L\uparrow$, is a function of needle temperature only so that:

$$\delta L\uparrow = \delta T(\partial L\uparrow/\partial T) \tag{25}$$

Since $L\uparrow = 0.9(0.97\ \sigma T^4)$ and $\delta T = 1°C$, equation 25 can be rewritten as:

$$\delta L\uparrow = 3.49\ \sigma T^3 \text{ W/m}^2 \tag{26}$$

where T is the needle temperature in degrees Kelvin. Evaluating $\delta L\uparrow$ at T = 303 K (30°C), gives a value of $\delta L\uparrow = 5.51$ W/m^2. Again, this value will not change much due to T being in Kelvin.

The error in Q* can now be rewritten as:

$$\delta Q^* = \{[2(0.7)(\delta V)(1/c)(\frac{1}{0.104 + \cos Z_s})]^2 + (6.8)^2 + (5.5)^2\}^{1/2} \quad (27)$$

using the values for δK, $\delta L\downarrow$, and $\delta L\uparrow$ as derived above. Calculations of δQ^*, given values for Z_s, GLOBAL, and Q* for seedling CN on August 7, 1981, are shown in Table D2. The relative probable error, $\delta Q^*/Q^*$, appears to be both constant, around 2%, and lower than the relative error in LE (Table D1). From equation 27 and Table D2 values of Q*, it is evident that the error in the longwave radiation determinations ($L\downarrow$ and $L\uparrow$) is the largest (~ 83%) component of error in Q*.

Error in Bowen Ratio

The error in the Bowen ratio can be calculated by first considering the functional relationship used in HEATDUMP: $\beta = (Q^* - LE)/LE$ so that the error in β is:

$$\delta\beta = [(\delta Q^* \frac{\partial\beta}{\partial Q^*})^2 + (\delta LE \frac{\partial\beta}{\partial LE})^2]^{1/2} \quad (28)$$

Using values of $\delta Q^*/Q^* = 2\%$ and $\delta LE/LE = 15\%$, and evaluating the differentials of β gives:

$$\delta\beta = [(0.02 \frac{Q^*}{LE})^2 + (0.15 \frac{LEQ^*}{LE^2})^2]^{1/2} \quad (29)$$

Calculations of β for seedling CN are shown in Table D3 for four days in the summer of 1981.

Error in Sensible Heat Flux

The sensible heat flux, H, was calculated by difference: $Q^* - LE$. The probable error in H, δH, therefore, is:

$$\delta H = [(\delta Q^*)^2 - (\delta LE)^2]^{1/2} \quad (30)$$

Since $\delta Q^* = 0.02\ Q^*$, and $\delta LE = 0.15\ LE$, δH can be rewritten as:

$$\delta H = [(0.02\ Q^*)^2 + (0.15\ LE)^2]^{1/2} \quad (31)$$

Calculations of error in H for four days are shown in Table D4 for seedling CN as an example.

APPENDIX D

Table D1. Relative probable error ($\delta LE/LE$) in seedling CN latent heat flux (LE) for given values of stomatal resistance (r_s) and vapor density deficit ($\rho^1 - \rho$).

r_s	$\rho^1 - \rho$	LE	δLE	$\delta LE/LE$
(s/cm)	(g/m^3)	------(W/m^2)-----		(%)
1	17.5	424	64.4	15
10	23.1	56	8.5	15
100	40.4	9.8	1.5	15
700	40.4	1.4	0.21	15

Table D2. Relative probable error ($\delta Q^*/Q^*$) in seedling CN net radiation (Q^*) for sun zenith angles (Z_s) and measured global radiation (GLOBAL) at four times on August 7, 1981.

Time	Z_s	GLOBAL	Q^*	δQ^*	$\delta Q^*/Q^*$
	(deg)	----------W/m^2----------			(%)
0900	48.3	605	397	9.0	2.3
1200	25.7	913	514	9.1	1.8
1500	43.8	758	526	9.1	1.7
1700	65.6	432	433	9.1	2.1

Table D3. Relative probable error ($\partial\beta/\beta$) in seedling CN Bowen ratio (β) for values of net radiation (Q*) and latent heat flux (LE) on four days in the summer of 1981.

Julian Date	Q*	LE	β	$\delta\beta$	$\delta\beta/\beta$
	----W/m^2----				(%)
148	204	13	14.7	2.4	16
185	149	9	15.6	2.5	16
219	193	6	31.2	4.9	16
239	193	3	63.3	9.7	15

Table D4. Relative probable error ($\partial H/H$) in seedling CN convective heat flux (H) for values of net radiation (Q*) and latent heat flux (LE) on four days in the summer of 1981.

Julian Date	Q*	LE	H	δH	$\delta H/H$
	----------W/m^2----------				(%)
148	204	13	191	4.5	2.4
185	149	9	140	3.3	2.4
219	193	6	187	4.0	2.1
239	193	3	190	3.9	2.0

REFERENCES CITED

Beardsell, M. F., P. G. Jarvis, and B. Davidson. 1972. A null-balance diffusion porometer suitable for use with leaves of many shapes. J. Appl. Ecol. 9:677-690.

Campbell, G. S. 1977. An Introduction to Environmental Biophysics. Springer-Verlag, New York. 159 pp.

Fritschen, L. J., and L. W. Gay. 1979. Environmental Instrumentation. Springer-Verlag, New York. 216 pp.

Gates, D. M. 1965. Energy, plants, and ecology. Ecology 46:1-13.

Gates, D. M., H. J. Keegan, J. C. Schleter, and V. R. Weidner. 1965. Spectral properties of plants. Applied Optics 4:11-30.

Gates, D. M., E. C. Tibbals, and F. Kreith. 1965. Radiation and convection for ponderosa pine. Amer. J. Bot. 52:66-71.

Holbo, H. R. 1973. Energy exchange studies at the earth's surface. II. Energy budget of a pumice desert. Oregon St. Univ. Dept. Atmos. Sci. Tech. Note. No. 73-II. 142 pp.

Idso, S. B., and R. D. Jackson. 1969. Thermal radiation from the atmosphere. J. Geophysical Research 74:5397-5403.

Jarvis, P. G., G. B. James, and J. J. Landsberg. 1976. 7. Coniferous forest. pp. 171-240 in Vegetation and the Atmosphere, Vol. 2, Case Studies, (ed.) J. L. Monteith, Academic Press, London, New York, San Francisco.

Monteith, J. L. 1973. Principles of Environmental Physics, Edward Arnold, London. 241 pp.

Norman, J. M., and P. G. Jarvis. 1974. Photosynthesis in Sitka spruce [Picea sitchensis (Bong.) Carr.]. III. Measurements of canopy structure and interception of radiation. J. Appl. Ecol. 11:375-398.

Peterson, W. A., and I. Dirmhirn. 1981. The ratio of diffuse to direct solar irradiance (perpendicular to the sun's rays) with clear skies - A conserved quantity throughout the day. J. Appl. Meteorol. 20:826-828.

Rao, C. R. N., T. Y Lee, W. A. Bradley, and D. Christopherson. 1982. Solar radiation and related meteorological data for Corvallis, Oregon - 1981. Oregon St. Univ. Dept. of Atm. Sci. Tech. Rep. No. 5. 227 pp.

Robinson, N. 1966. Solar Radiation. Elsevier Publ. Co. 347 pp.

Scarborough, J. B. 1966. Numerical Mathematical Analysis. The Johns Hopkins Press, Baltimore, MD. 600 pp.

Tibbals, E. C., E. K. Carr, D. M. Gates, and F. Kreith. 1964. Radiation and convection in conifers. Amer. J. Bot. 51:529-538.

Woolley, J. T. 1971. Reflectance and transmittance of light by leaves. Plant Physiol. 47:656-662.